ORNL/SPR-2023/3164

Mechanical Properties of Neutron-Irradiated Zr-Alloy Weldments (Batch #2)

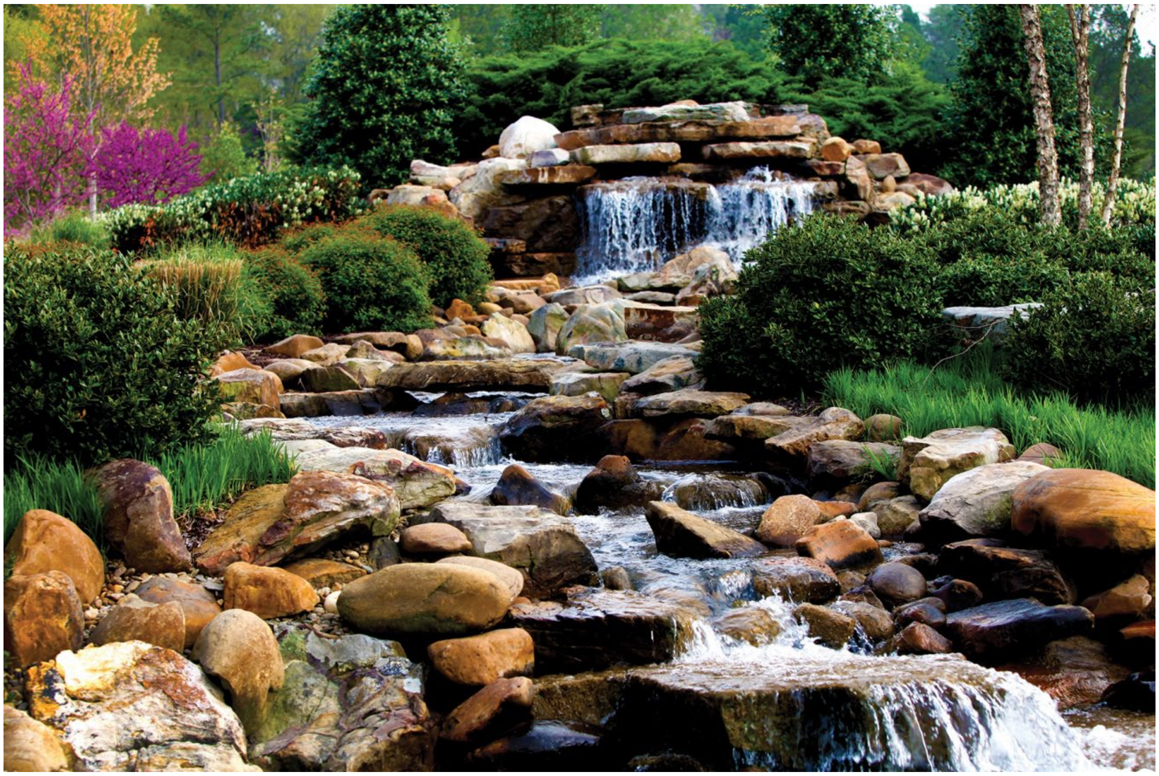

M. Gussev
X. Chen
T Dixon
J. Harp

October 2023

ORNL IS MANAGED BY UT-BATTELLE LLC FOR THE US DEPARTMENT OF ENERGY

ORNL/SPR-2023/3164

Nuclear Energy and Fuel Cycle Division
Materials Science and Technology Division

MECHANICAL PROPERTIES OF NEUTRON-IRRADIATED ZR-ALLOY WELDMENTS (BATCH #2)

M. Gussev
X. Chen
T. Dixon
J. Harp

October 2023

Prepared by
OAK RIDGE NATIONAL LABORATORY
Oak Ridge, TN 37831
managed by
UT-BATTELLE LLC
for the
US DEPARTMENT OF ENERGY
under contract DE-AC05-00OR22725

CONTENTS

LIST OF FIGURES

LIST OF TABLES

ABBREVIATIONS

HAZ	heat-affected zone
LAMDA	Low Activation Materials Development and Analysis
ORNL	Oak Ridge National Laboratory
TE	total elongation
UE	uniform elongation
UTS	ultimate tensile stress
YS	yield stress

1. INVESTIGATED MATERIALS AND EXPERIMENTAL METHODS

This report summarizes the experimental results on microstructure, microhardness, and mechanical properties of Zr alloy weldments irradiated by neutrons.

1.1 LIST OF MATERIALS

Nine irradiated specimens (i.e., weldments) were shipped from the Oak Ridge National Laboratory (ORNL) Irradiated Material Examination and Testing Facility to the Low Activation Materials Development and Analysis (LAMDA) laboratory for mechanical testing. Table 1 lists the specimens along with their weld microstructures.

Table 1. List of specimens with microstructure types for Vickers hardness measurements and mechanical testing

Specimen ID	Weld microstructure	Irradiated (Y or N)	Nominal dimension (mm)
61-7143	Blocky Alpha	Y	21 (L) × 5 (W) × 3.25 (T)
61-7180	Blocky Alpha	Y	
61-7181	Blocky Alpha	Y	
61-7194	Blocky Alpha	Y	
61-7270	Precursor	Y	
61-7279	Precursor	Y	
61-7284	Precursor	Y	
61-7304	Precursor	Y	
61-7357	Widmanstätten	Y	

The representative cross-sectional images for the Widmanstätten, Blocky Alpha, and Precursor weld microstructures are shown in Figures 1–3.

Figure 1. Widmanstätten weld microstructure. Red lines indicating the end of the heat-affected zone (HAZ).

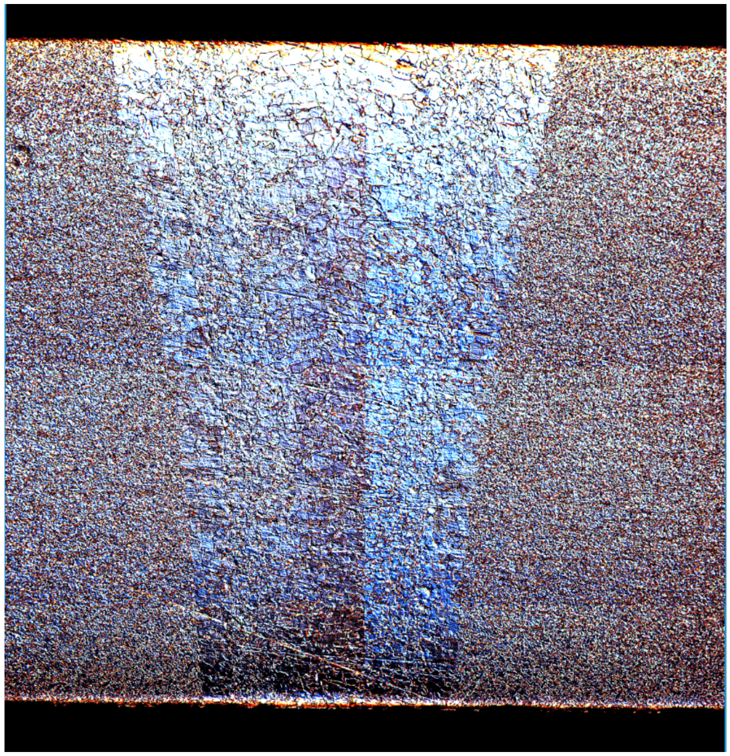

Figure 2. Blocky alpha weld microstructure.

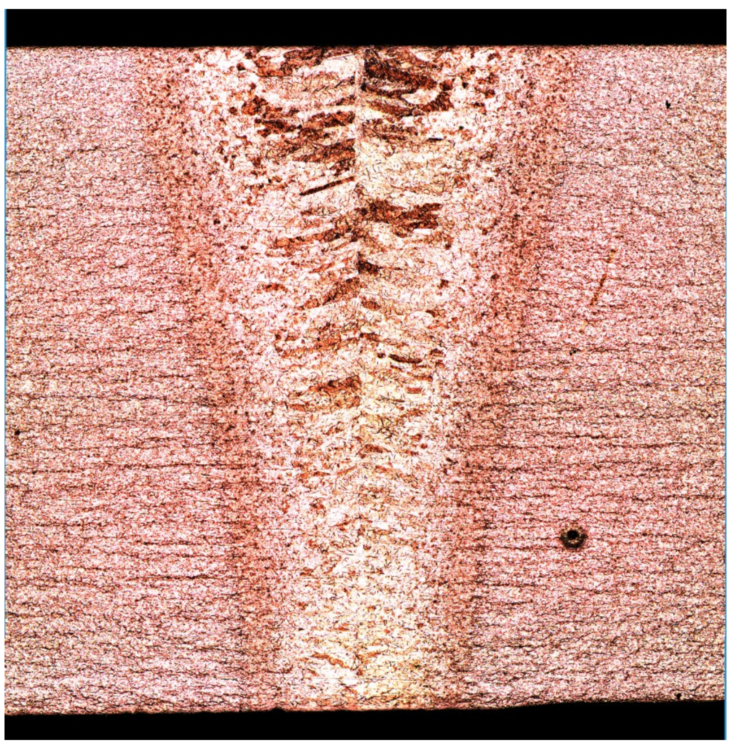

Figure 3. Precursor weld microstructure.

Similar to the Batch #1 test specimens, all Batch #2 test specimens were beam shaped and had nominal dimensions of 21 mm × 5 mm × 3.25 mm, as shown in Figure 4. The weld was positioned in the center of the 21.0 mm dimension and penetrated the 5.0 mm dimension. Each test specimen was engraved with a unique ID. A sample image for one of the tested specimens is shown in Figure 5.

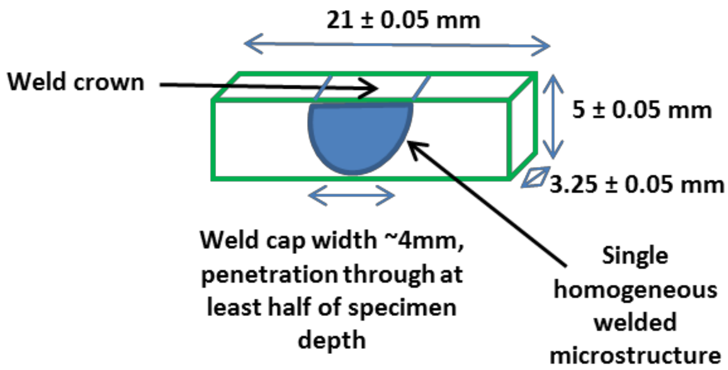

Figure 4. Schematic drawing of test specimen geometry.

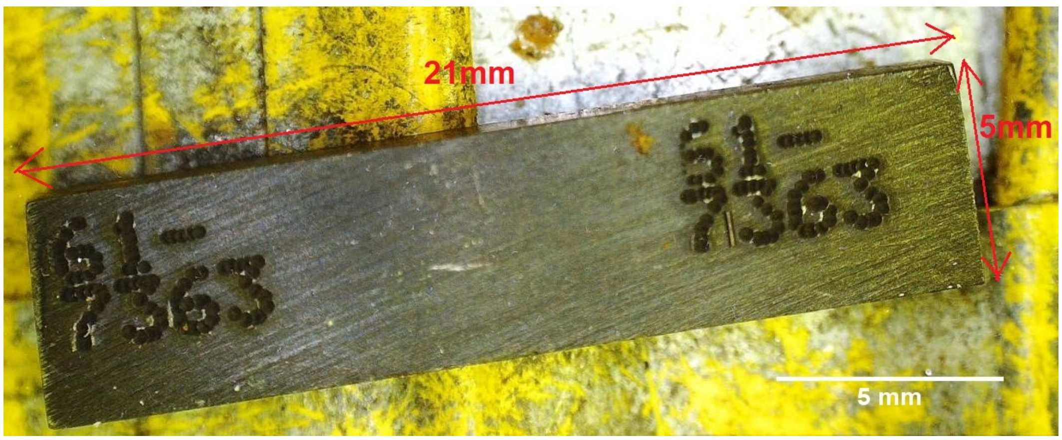

Figure 5. Sample image for specimen 61-7363.

1.2 HARDNESS TESTING PROCEDURES

Before Vickers hardness testing was performed, each specimen's top and side surfaces were polished with a 2500 grit finish and then swabbed with an etching solution of 60 mL water, 35 mL nitric acid, and 5 mL hydrofluoric acid to reveal the weld microstructure. The Vickers hardness tester used was a Wilson model VH3100 manufactured by Buehler. Hardness testing was performed at 500 gf with a 10 s dwell time. Before testing irradiated specimens, two hardness standard blocks (i.e., HV160 gf–HV500 gf and HV300 gf–HV500 gf) were used to verify that the hardness tester was in a good working condition. Hardness testing was then performed on the top and side surfaces of each specimen, according to the indentation pattern preapproved by the sponsor.

1.3 TENSILE SPECIMEN GEOMETRY

A miniature SS-Mini tensile specimen was used for the Batch #2 specimen testing; this specimen has a gauge with dimensions of 3.55 mm (length) × 0.8 mm (width) × 0.4 mm (thickness). This geometry (Figure 6) was designed to evaluate the engineering mechanical properties of small objects, such as weldments, with inhomogeneous structure and property gradients [1]. This geometry is similar to more common SS-J geometry [2], but it has much smaller dimensions. The SS-Mini specimens were used for testing advanced materials, such as FeCrAl alloys, and their weldments [3,4].

For the wrought materials, the SS-Mini geometry provides results similar to those of the SS-J specimen [1]. Shoulder-loading grips (Figure 7) were used during mechanical testing, and the grips are made of precipitation-hardened 718 alloy, providing sufficient strength and carrying capacity.

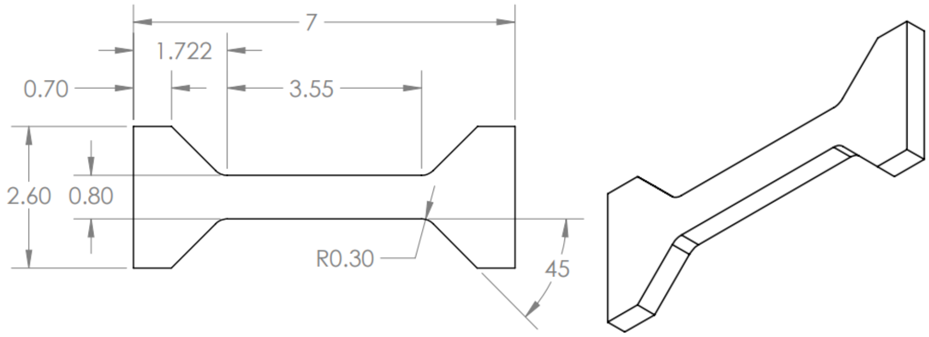

Figure 6. The shape and geometry of the selected tensile specimen. The specimen thickness could be 0.4 mm or 0.6 mm, depending on the material availability. The 0.4 mm thickness was adopted for the present project to allow for more specimens to be manufactured and tested.

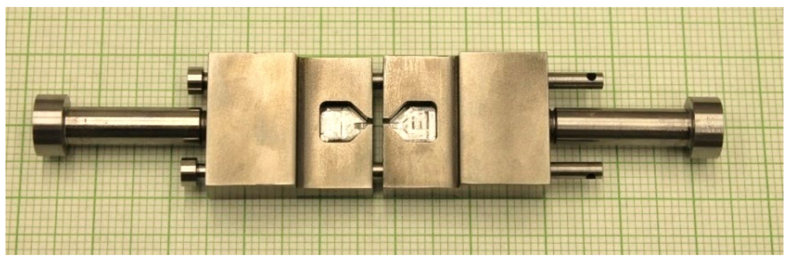

Figure 7. Grips for mechanical testing.

1.4 SPECIMEN MANUFACTURING AND PREPARATION

Tensile specimens were manufactured using high-precision, industrial-scale electric discharge machine (EDM) installed in the LAMDA facility. During manufacturing, the 3.25 mm blanks with SS-Mini geometry were cut from the welded coupons. The blanks were sliced into ~0.6 mm tensile objects, providing ~0.2 mm of extra thickness for mechanical grinding and preparation. Afterward, the cut objects were mechanically grinded and polished down to 0.4 mm (nominal SS-Mini specimen thickness) with 1200 grit sandpaper.

Figure 8 shows the tensile specimen location and orientation, with respect to the welded coupon. The goal was to “fit” the weldment precisely into the gauge section.

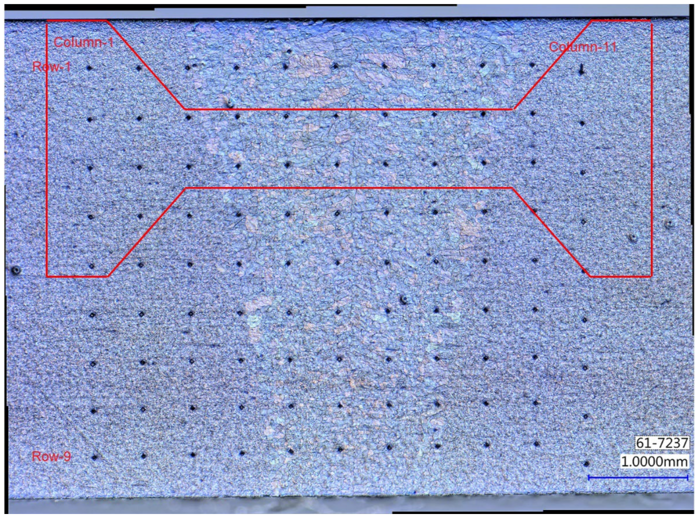

Figure 8. Tensile specimen location and orientation (with respect to the weldment), showing how the weldment "fits" into the tensile specimen gauge.

Also, an additional set of specimens was manufactured from the weld bottom. In this case, the specimens were cut differently. The orientation was changed to ensure the specimen integrity (Figure 9).

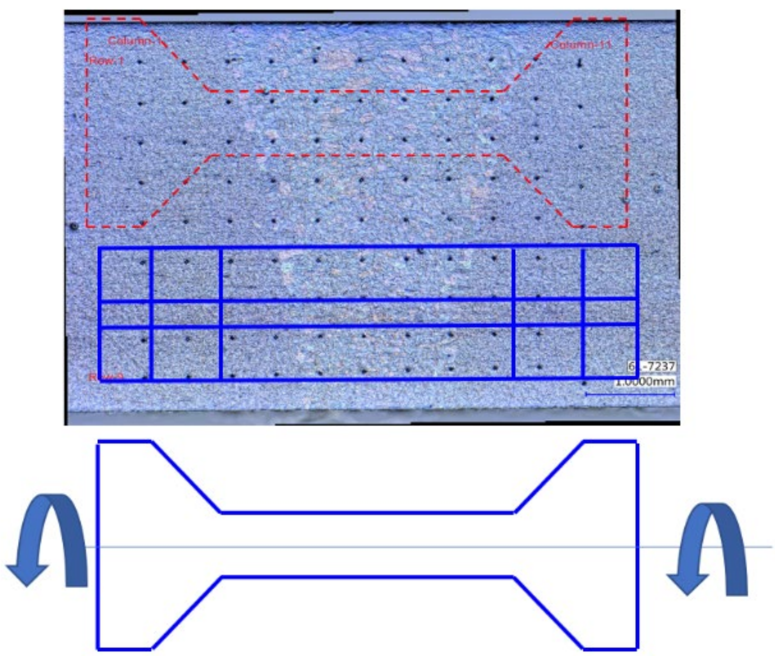

Figure 9. Location and orientation of additional specimens (blue outline) cut from the weldment bottom portion.

1.5 MECHANICAL TESTING

The tests were performed using a 2kN MTS (Material Testing System) electromechanical single-column tensile frame. A custom temperature cabinet—designed and manufactured by ATS (Applied Test Systems, Inc.), was installed on the frame and used for tests at elevated temperatures. The intended strain rate was ~0.001 s^{-1} (displacement rate of 0.213 mm/min); however, a subset of specimens was tested at an elevated strain rate (~0.01 s^{-1}, or a displacement rate of 2.13 mm/min).

2. RESULTS

2.1 MICROHARDNESS MEASUREMENTS AND MAPPING

Vickers hardness results from irradiated Zr weld specimens are listed in Tables 2–10, and the corresponding indentation images are shown in Figures 10–18.

Table 2. Specimen 61-7143 Vickers hardness results

Surface	Indentation row #	Indentation column #											
		1	2	3	4	5	6	7	8	9	10	11	12
Top	1	248	273	256	232	262	250	257	273	257	278	269	249
Side	1	220	231	225	233	233	239	240	236	221	228	230	227
	2	236	227	231	228	245	256	226	231	224	222	232	222
	3	225	225	228	228	236	245	240	228	239	221	229	229
	4	225	230	220	221	220	246	274	240	257	229	218	227
	5	226	227	221	230	222	221	234	229	259	213	237	218
	6	218	218	221	233	230	235	309	277	256	238	225	229
	7	221	224	227	220	236	246	241	236	250	216	220	225
	8	219	221	224	234	221	229	245	250	238	226	230	226
	9	230	228	227	226	233	NA*	237	263	252	220	220	229

*Indent hit a surface cavity
NA = not applicable

Table 3. Specimen 61-7180 Vickers hardness results

Surface	Indentation row #	Indentation column #											
		1	2	3	4	5	6	7	8	9	10	11	12
Top	1	243	257	256	249	243	233	245	262	239	278	249	257
Side	1	222	225	225	256	267	266	274	286	240	226	223	223
	2	228	223	224	233	224	236	272	240	275	231	235	220
	3	223	231	218	230	229	234	232	252	231	230	226	227
	4	210	222	219	211	248	244	242	254	235	202	220	223
	5	228	221	222	228	232	255	252	233	248	225	228	234
	6	221	226	216	225	230	279	252	268	227	230	228	210
	7	214	223	224	231	223	243	250	241	236	220	224	226
	8	226	226	203	224	240	260	267	247	219	217	220	229
	9	220	222	237	228	217	269	266	241	229	229	238	221

Table 4. Specimen 61-7181 Vickers hardness results

Surface	Indentation row #	Indentation column #											
		1	**2**	**3**	**4**	**5**	**6**	**7**	**8**	**9**	**10**	**11**	**12**
Top	1	261	252	271	235	247	227	245	239	244	248	247	253
Side	1	232	221	226	272	230	236	238	249	247	219	223	225
	2	218	225	226	236	260	240	229	254	228	220	225	225
	3	219	221	239	223	253	245	240	240	272	223	231	223
	4	242	230	226	229	246	245	238	244	283	239	232	228
	5	231	238	223	223	220	251	262	277	225	235	228	219
	6	225	223	221	229	226	247	266	243	223	228	226	224
	7	226	222	231	237	231	260	260	226	221	230	235	234
	8	219	224	221	227	225	235	245	246	226	228	226	223
	9	235	226	225	228	223	269	265	235	221	232	234	237

Table 5. Specimen 61-7194 Vickers hardness results

Surface	Indentation row #	Indentation column #											
		1	**2**	**3**	**4**	**5**	**6**	**7**	**8**	**9**	**10**	**11**	**12**
Top	1	251	256	255	230	237	245	234	237	257	220	249	254
Side	1	228	230	232	263	252	259	259	267	253	227	225	226
	2	234	224	229	232	242	238	236	260	262	247	224	227
	3	229	212	224	225	251	243	219	249	250	219	239	234
	4	242	231	226	229	225	244	257	250	243	222	219	221
	5	224	224	225	227	233	238	248	278	233	228	223	234
	6	232	223	224	224	228	232	243	253	282	225	234	224
	7	221	225	232	223	228	276	255	247	224	230	229	220
	8	231	241	223	237	223	238	285	266	231	232	233	221
	9	224	224	222	223	231	220	248	255	228	233	226	223

Table 6. Specimen 61-7270 Vickers hardness results

Surface	Indentation row #	Indentation column #											
		1	**2**	**3**	**4**	**5**	**6**	**7**	**8**	**9**	**10**	**11**	**12**
Top	1	268	256	275	275	303	309	309	285	296	290	277	281
Side	1	236	234	236	246	296	301	284	288	293	288	226	243
	2	231	226	222	221	289	319	299	290	307	280	223	213
	3	231	225	246	227	290	286	318	292	312	286	226	246
	4	223	228	228	246	282	282	311	288	307	262	223	226
	5	236	234	224	232	246	291	304	310	297	232	237	231
	6	226	230	243	224	223	301	297	303	299	229	221	218
	7	224	221	232	226	232	276	298	302	278	230	238	240
	8	239	227	233	230	233	295	318	305	270	237	235	238
	9	231	224	220	237	228	283	324	304	276	237	231	238

Table 7. Specimen 61-7279 Vickers hardness results

Surface	Indentation row #	Indentation column #											
		1	2	3	4	5	6	7	8	9	10	11	12
Top	1	257	258	271	262	296	297	294	300	311	298	275	254
Side	1	232	238	232	282	298	305	325	289	225	238	224	240
	2	238	231	231	295	299	297	298	299	238	243	226	222
	3	223	242	228	275	300	310	303	286	232	227	226	234
	4	227	236	221	254	309	300	303	271	226	231	233	228
	5	229	223	224	224	290	310	316	280	238	236	241	228
	6	232	232	233	231	302	306	304	267	221	217	233	235
	7	221	225	232	235	295	326	310	253	225	228	251	236
	8	234	228	225	238	304	306	318	249	232	232	230	234
	9	226	240	224	228	301	314	318	232	232	236	231	231

Table 8. Specimen 61-7284 Vickers hardness results

Surface	Indentation row #	Indentation column #											
		1	2	3	4	5	6	7	8	9	10	11	12
Top	1	252	252	261	265	287	333	295	292	300	279	NA*	276
Side	1	237	234	227	230	294	297	304	300	302	281	229	238
	2	237	231	237	233	287	296	284	308	285	239	229	237
	3	232	228	229	241	284	300	302	314	286	243	240	235
	4	236	232	233	228	292	318	314	307	294	228	229	234
	5	245	228	243	233	275	310	301	311	281	237	235	232
	6	239	234	235	235	241	306	315	305	270	242	230	227
	7	229	228	226	226	231	296	313	320	247	242	235	237
	8	229	225	229	239	231	307	327	309	238	233	235	233
	9	232	230	235	232	241	292	310	315	230	233	239	237

*Indent hit a surface cavity
NA = not applicable

Table 9. Specimen 61-7304 Vickers hardness results

Surface	Indentation row #	Indentation column #											
		1	2	3	4	5	6	7	8	9	10	11	12
Top	1	268	263	273	294	300	323	287	302	277	264	273	267
Side	1	228	235	247	282	290	287	296	282	243	215	229	211
	2	215	227	247	302	299	297	308	294	257	226	222	239
	3	228	235	225	298	293	297	297	302	245	227	217	229
	4	224	230	231	294	300	312	316	293	231	234	233	231
	5	237	228	219	276	314	304	308	279	226	231	239	240
	6	235	236	227	278	306	296	305	280	233	236	234	233
	7	244	230	226	260	302	304	310	267	223	236	227	228
	8	225	219	227	244	299	313	291	255	240	217	230	224
	9	233	226	227	224	295	312	310	227	224	231	219	234

Table 10. Specimen 61-7357 Vickers hardness results

Surface	Indentation row #	Indentation column #																		
		1	**2**	**3**	**4**	**5**	**6**	**7**	**8**	**9**	**10**	**11**	**12**	**13**	**14**	**15**	**16**	**17**	**18**	**19**
Top	1	273	250	273	253	239	242	243	268	242	233	224	232	256	257	224	238	252	226	226
Side	1	222	236	225	240	234	266	238	260	238	239	280	239	255	254	252	247	–	–	–
	2	232	226	230	252	246	256	267	245	252	253	243	244	250	250	236	251	–	–	–
	3	240	229	232	237	256	227	245	266	257	254	244	233	231	241	243	245	–	–	–
	4	228	229	234	250	265	245	250	263	238	262	263	234	249	234	226	243	–	–	–
	5	226	225	233	270	245	253	253	251	244	260	259	272	320	249	252	236	–	–	–
	6	235	227	232	245	245	261	250	250	243	254	239	241	231	293	233	244	–	–	–
	7	244	235	232	239	267	254	245	251	255	247	266	247	253	240	252	256	–	–	–
	8	231	235	233	255	254	242	264	256	246	249	252	250	277	239	251	252	–	–	–
	9	237	231	229	246	249	258	235	265	256	250	249	240	255	244	243	255	–	–	–

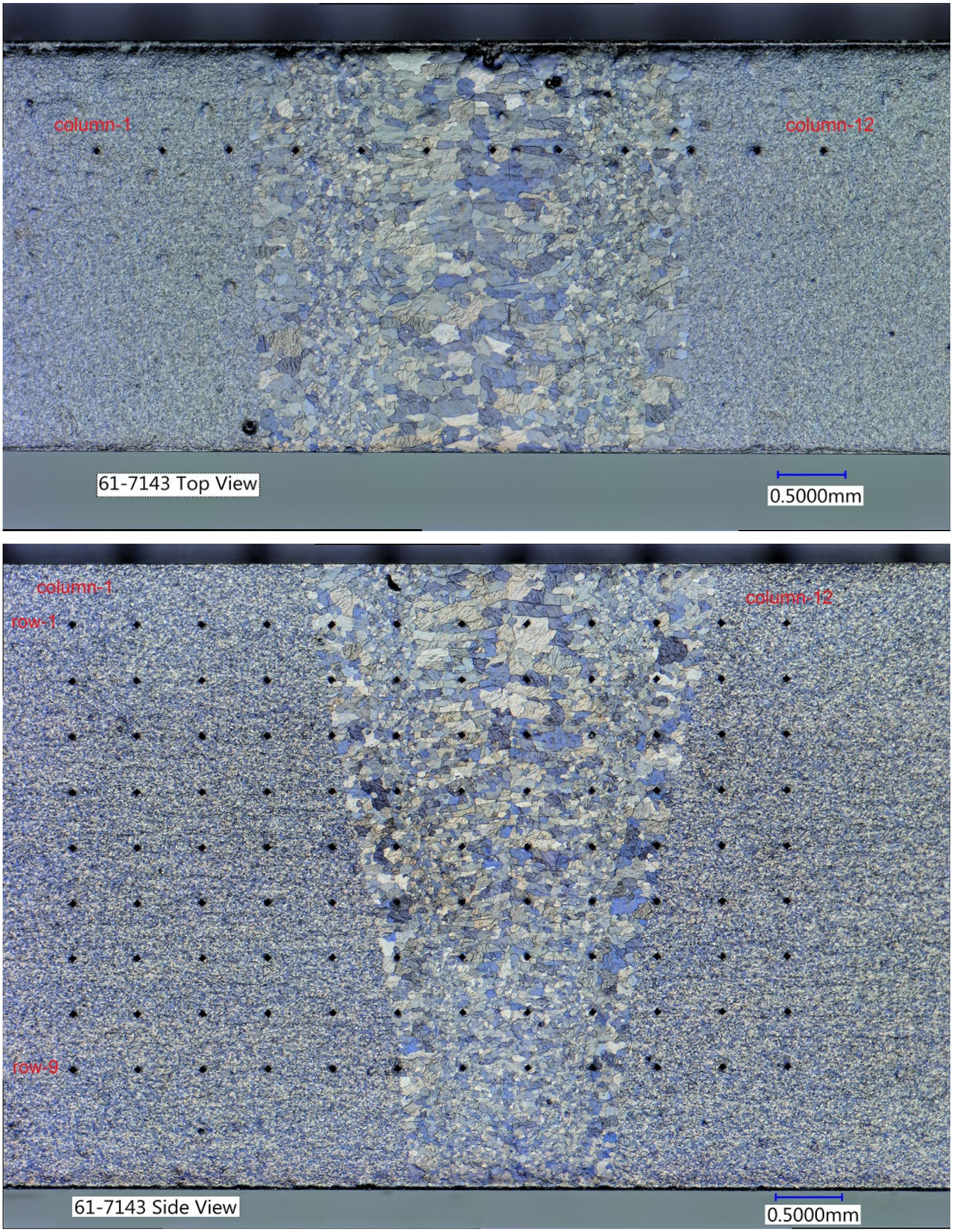

Figure 10. Optical images of hardness indentation from the top and side surfaces for specimen 61-7143.

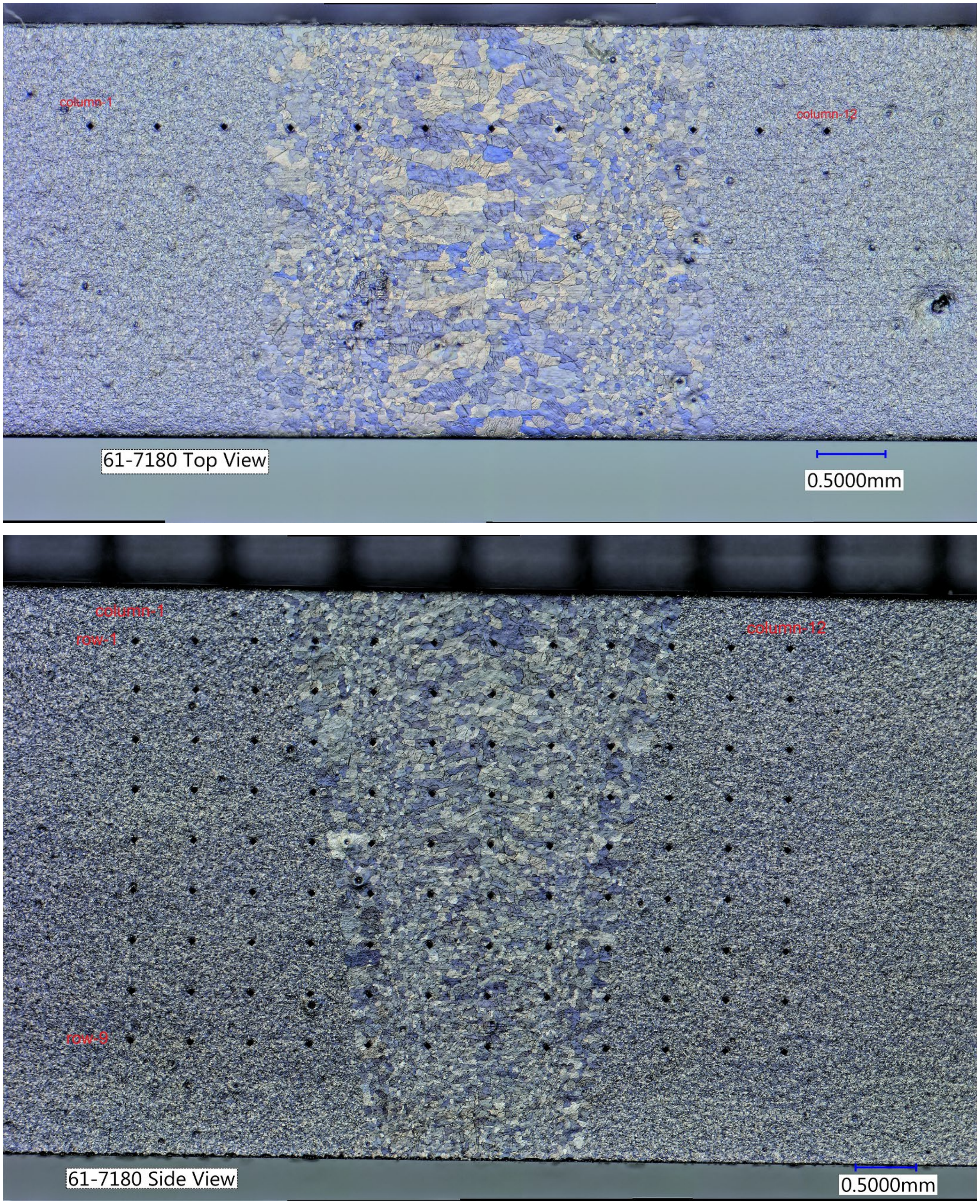

Figure 11. Optical images of hardness indentation from the top and side surfaces for specimen 61-7180.

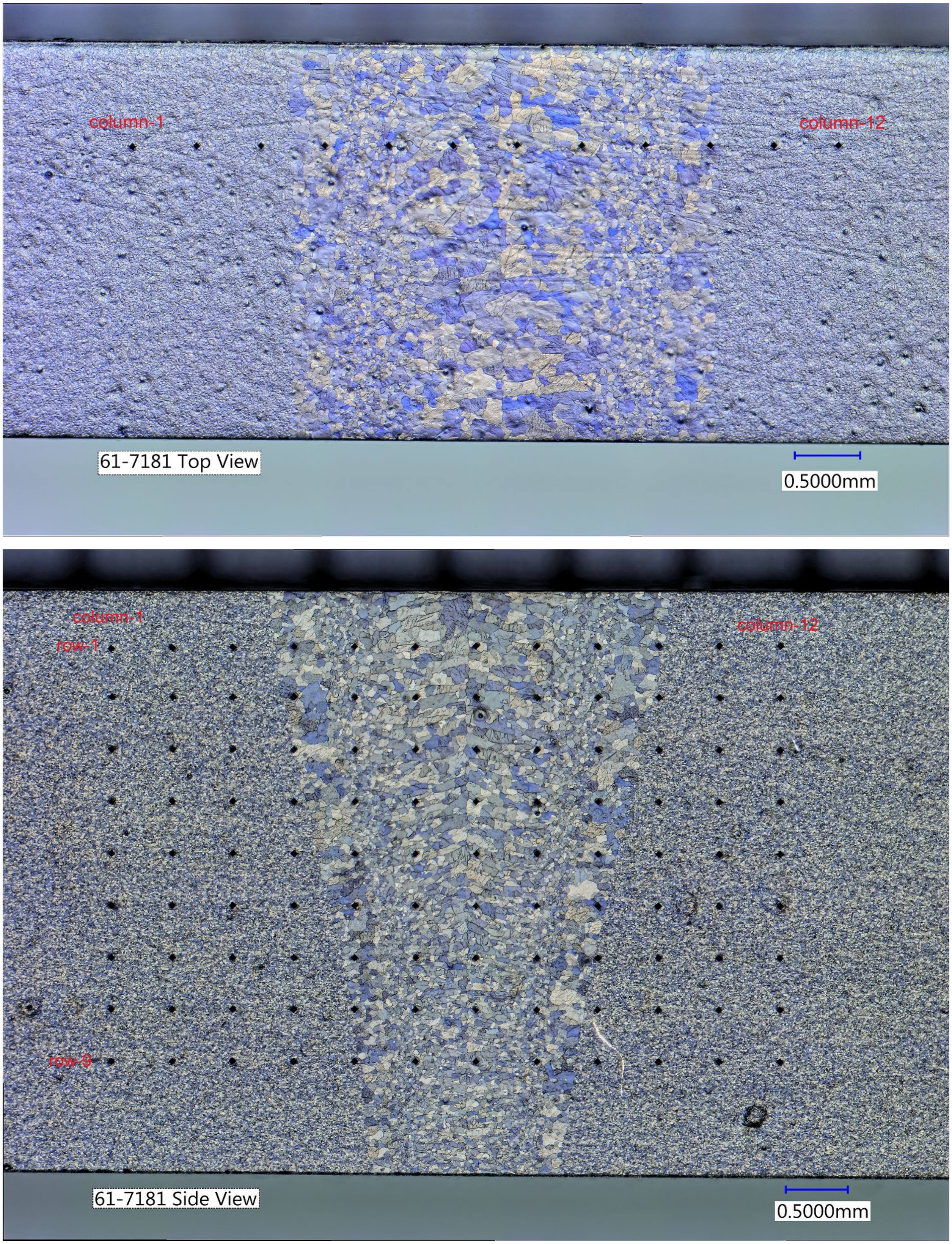

Figure 12. Optical images of hardness indentation from the top and side surfaces for specimen 61-7181.

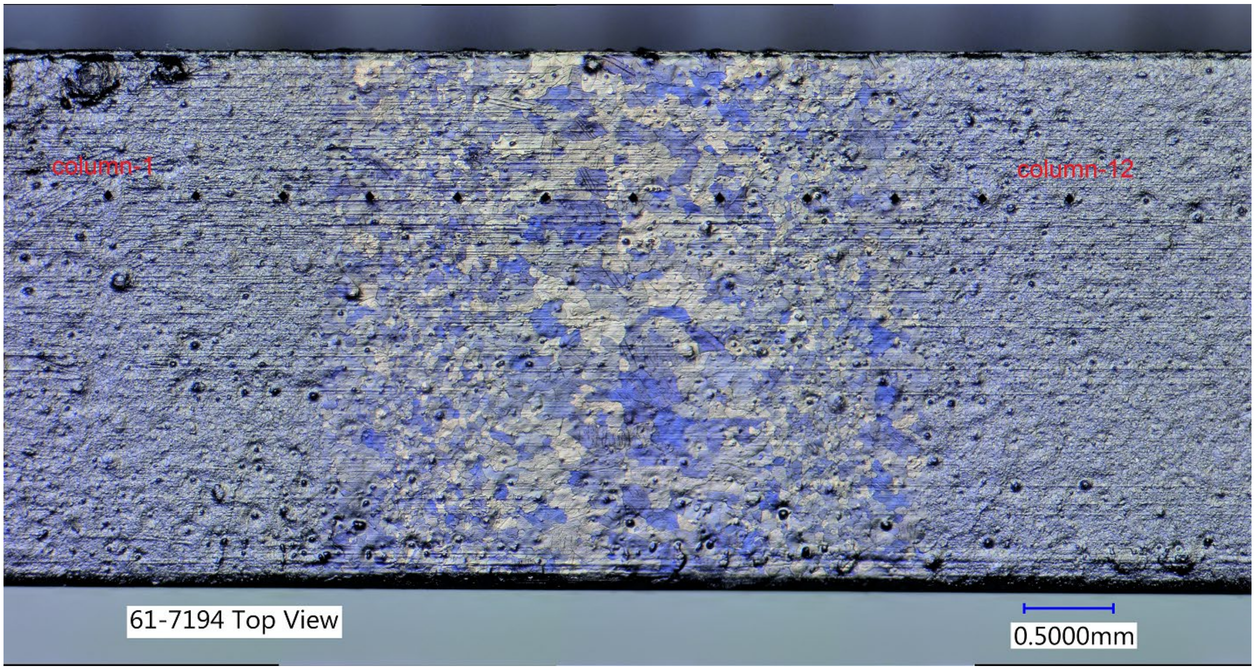

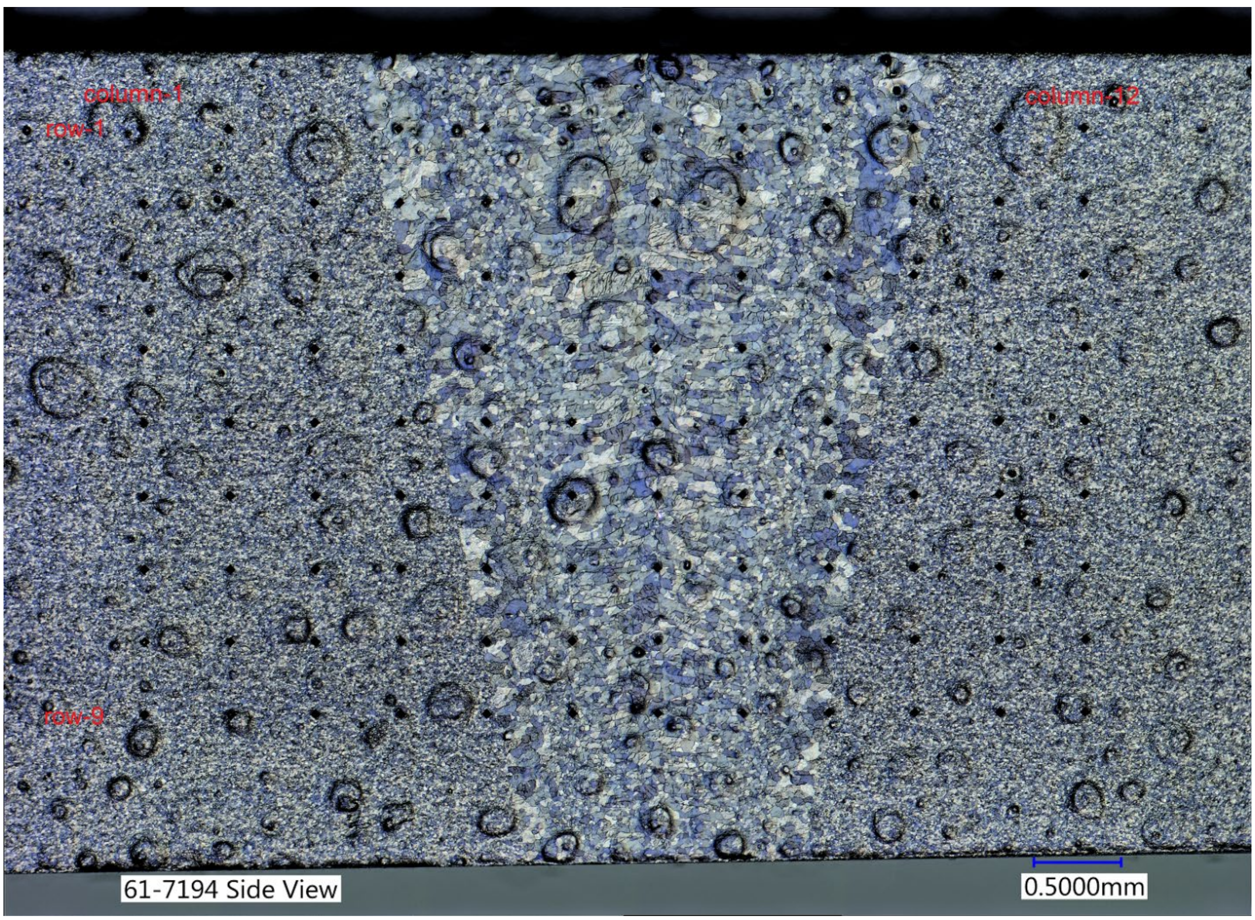

Figure 13. Optical images of hardness indentation from the top and side surfaces for specimen 61-7194.

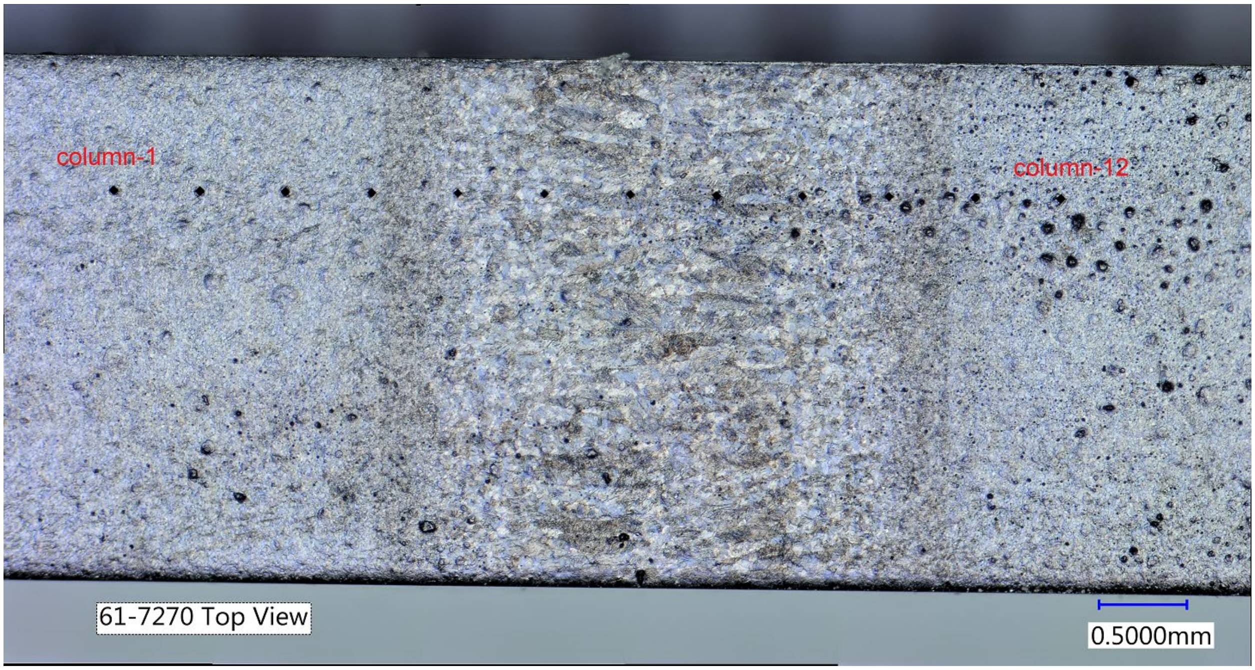

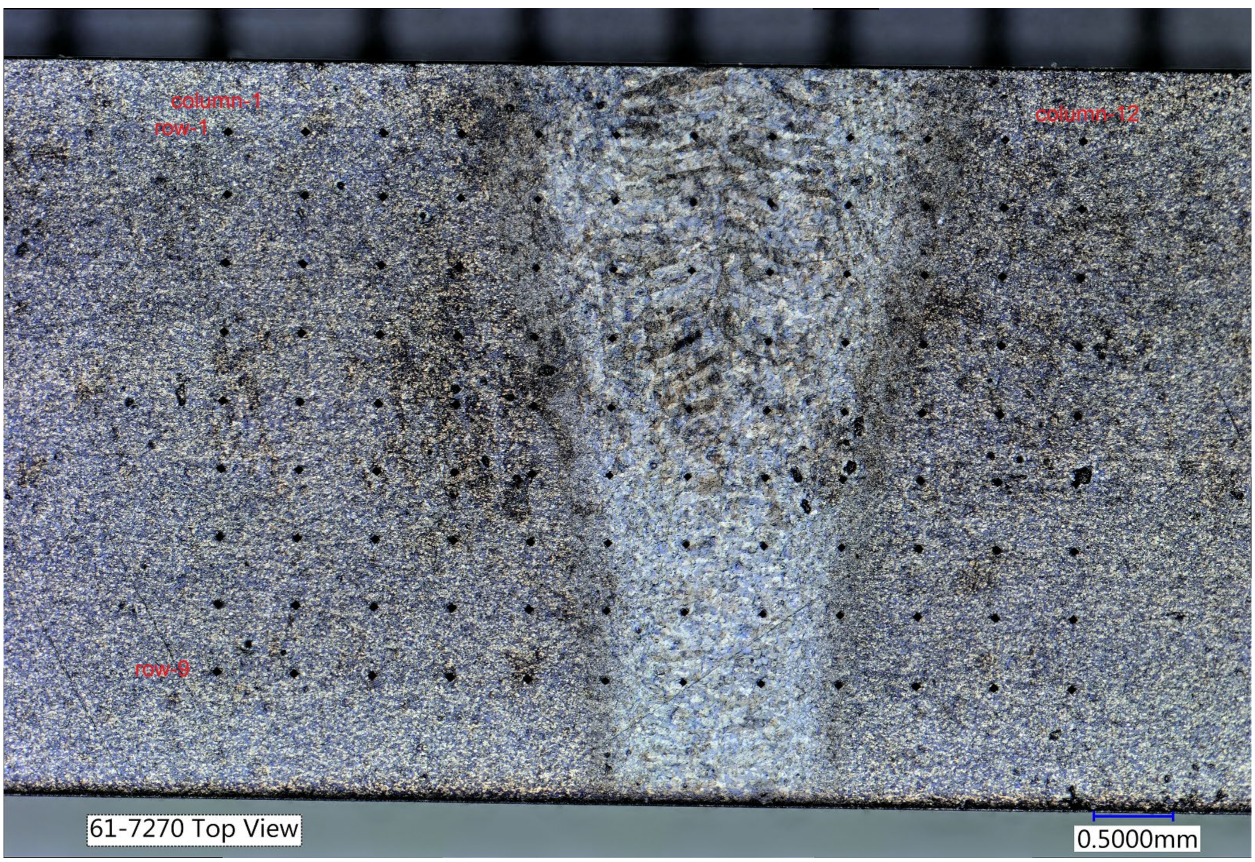

Figure 14. Optical images of hardness indentation from the top and side surfaces for specimen 61-7270.

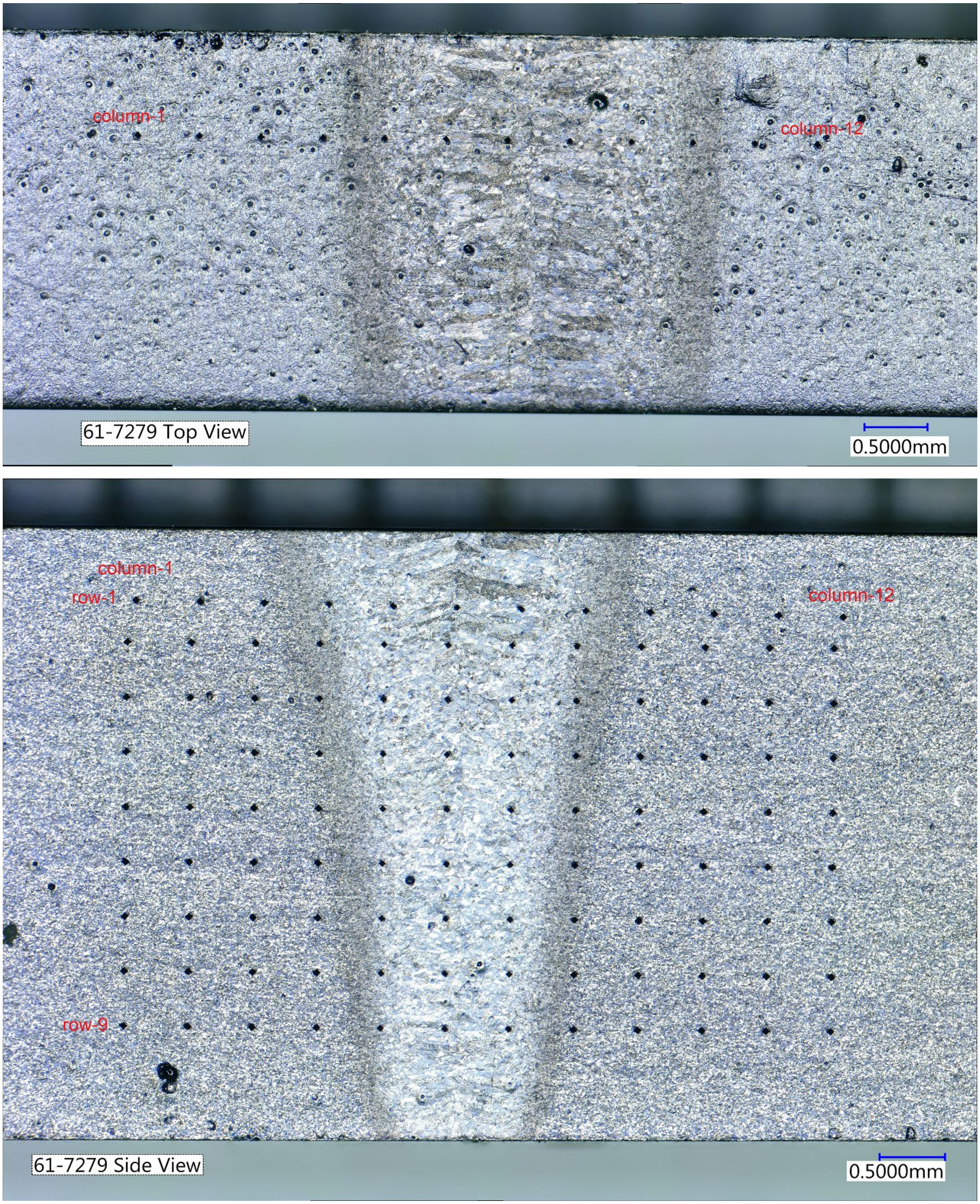

Figure 15. Optical images of hardness indentation from the top and side surfaces for specimen 61-7279.

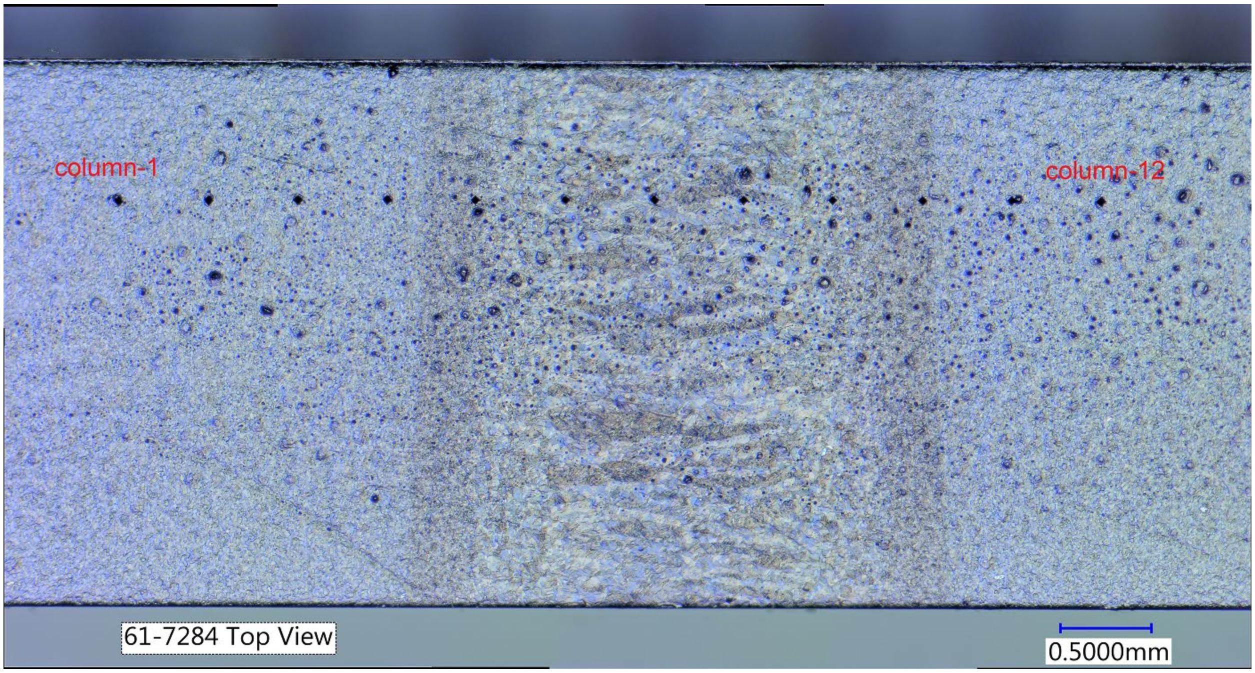

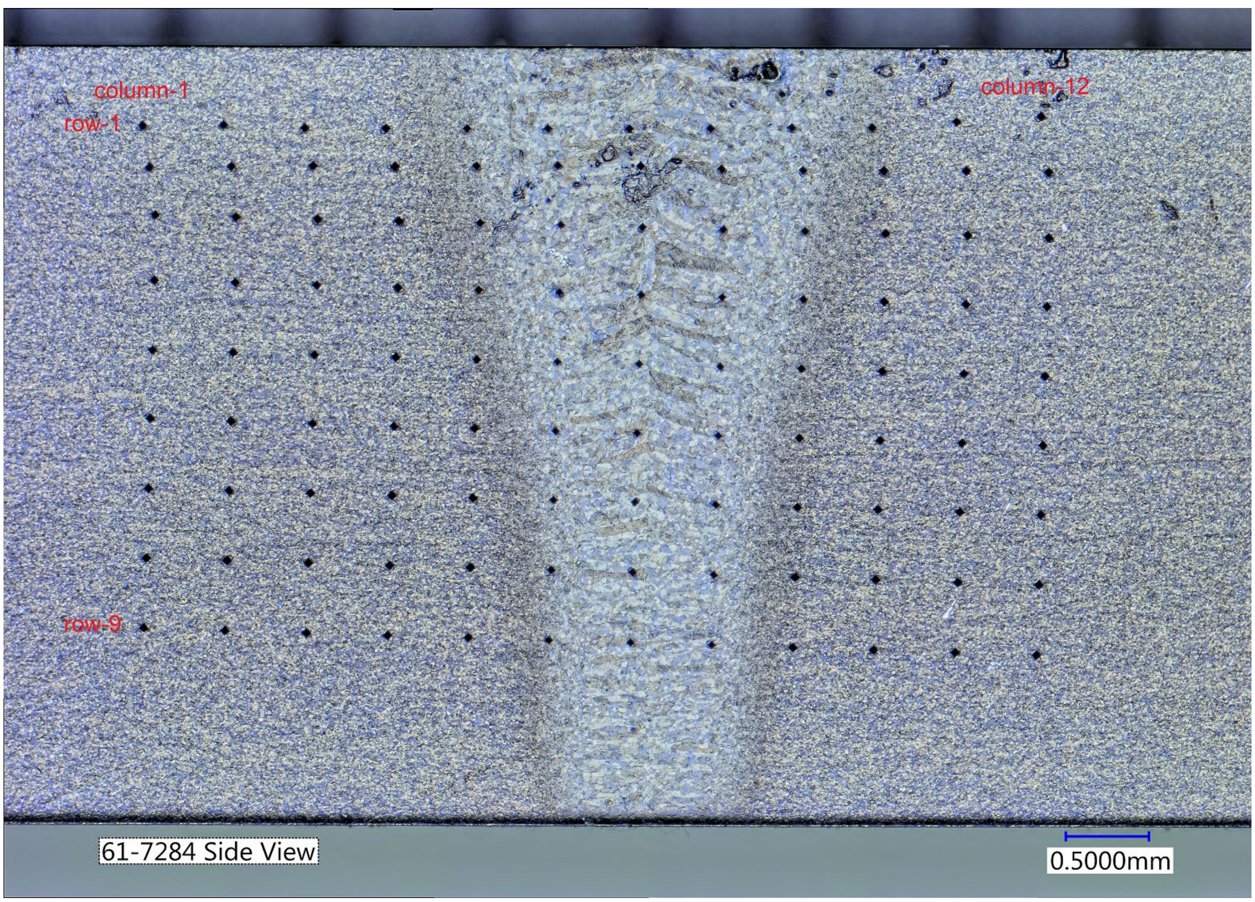

Figure 16. Optical images of hardness indentation from the top and side surfaces for specimen 61-7284.

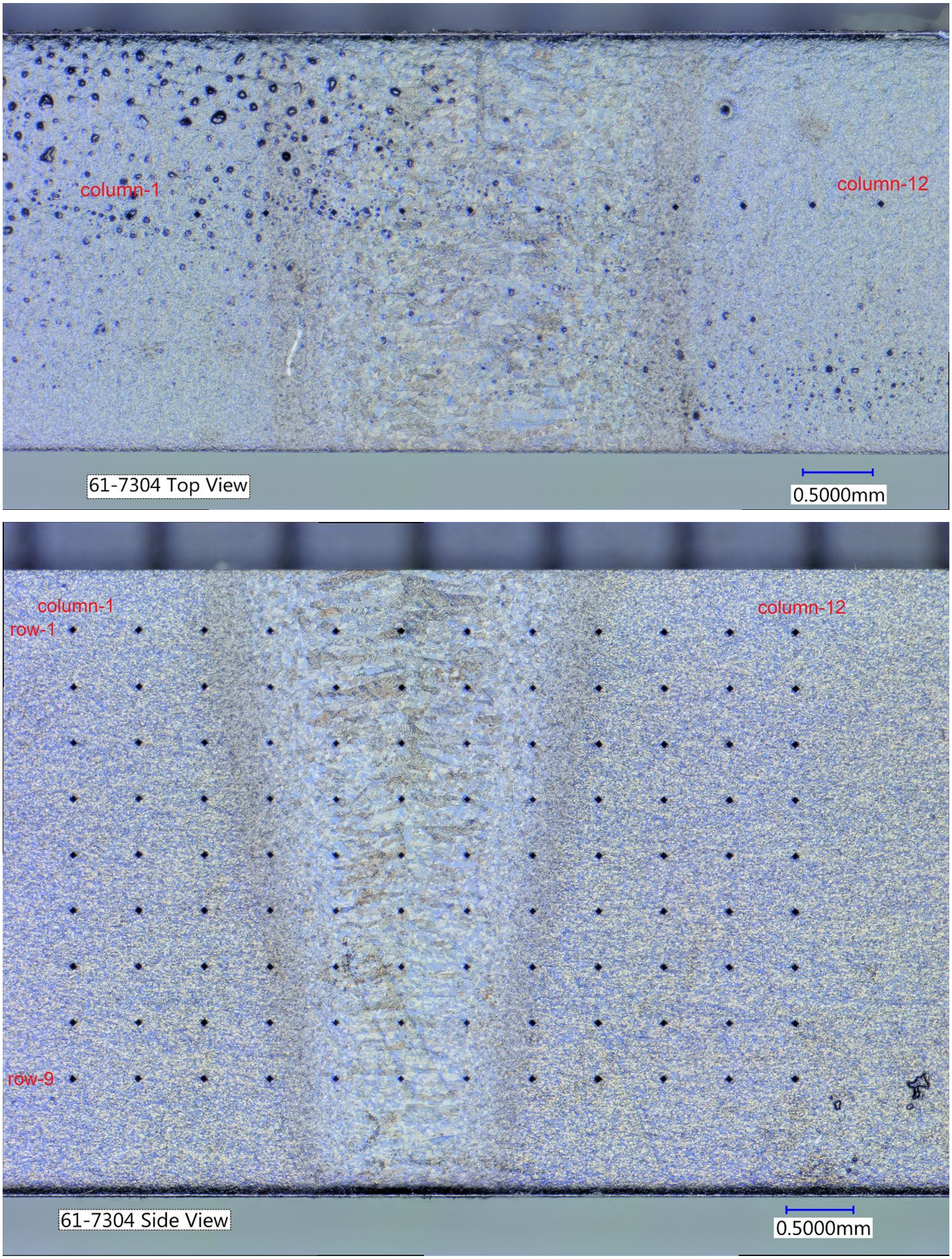

Figure 17. Optical images of hardness indentation from the top and side surfaces for specimen 61-7304.

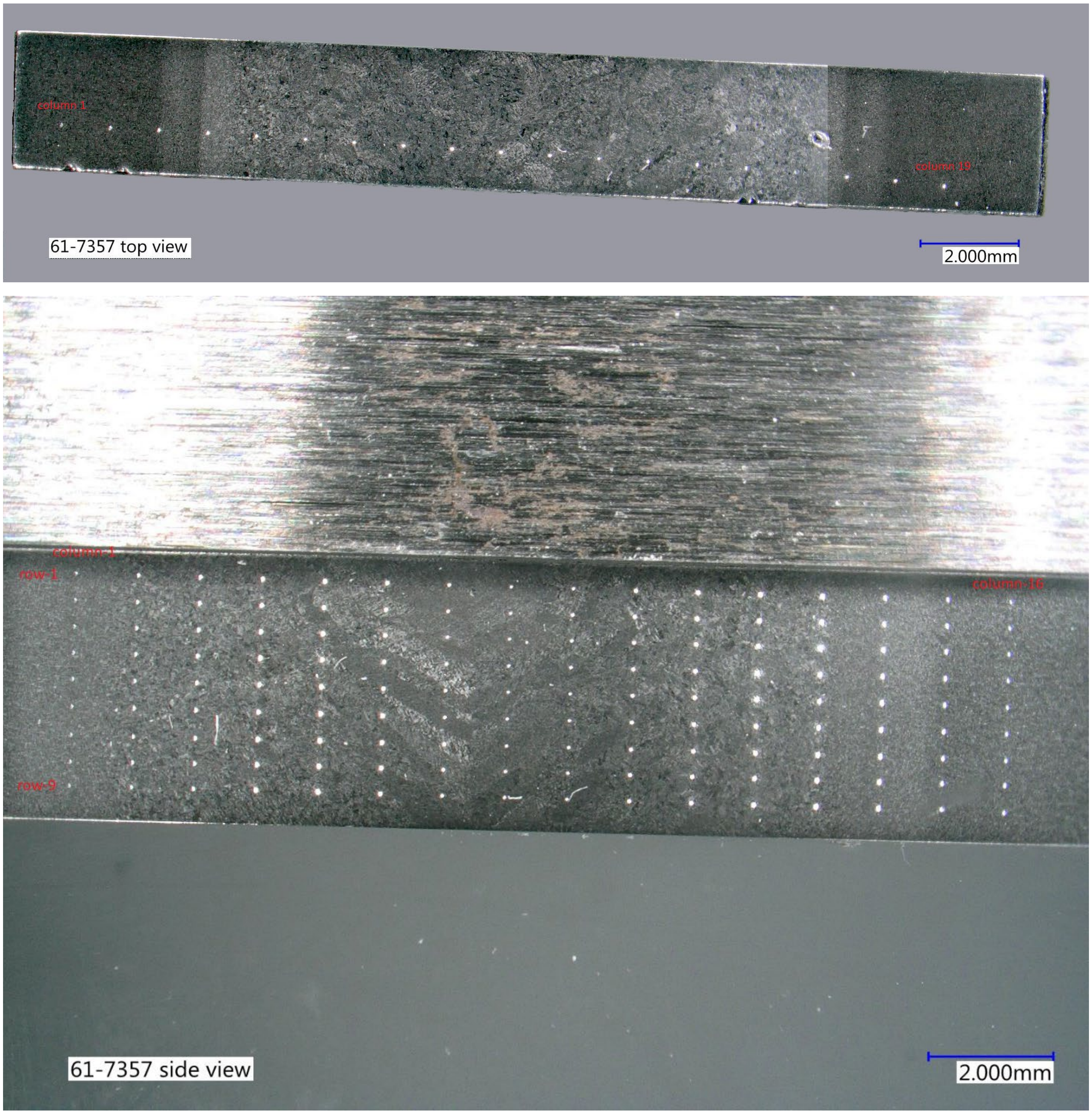

Figure 18. Optical images of hardness indentation from the top and side surfaces for specimen 61-7357.

To evaluate the hardness distribution on the top and side surfaces of each specimen, hardness distribution profiles were plotted for each specimen, and each weld fusion zone was superimposed on the profile maps; these profiles are shown in Figures 19–27. Observations for individual specimens are as follows.

1) **Specimens 61-7143, 61-7180, 61-7181, and 61-7194 with blocky alpha weld microstructure.** The weld crown on the top surface had similar hardness to that observed in the surrounding base metal. The weld fusion zone had higher hardness on the side surface than the surrounding base metal, with some degree of scattering in hardness for the weld fusion.

2) **Specimens 61-7270, 61-7279, 61-7284, and 61-7304 with precursor weld microstructure.** The weld fusion zone had higher hardness than that of the surrounding base metal, with the hardness peak typically centered in the weld fusion zone.

3) **Specimen 61-7357 with Widmanstätten weld microstructure.** A larger fluctuation in hardness was observed within the weld fusion and heat-affected zones (HAZs). The hardness from the weld fusion and HAZs was similar to the base metal hardness on one side, but it was higher than the base metal hardness on the other side.

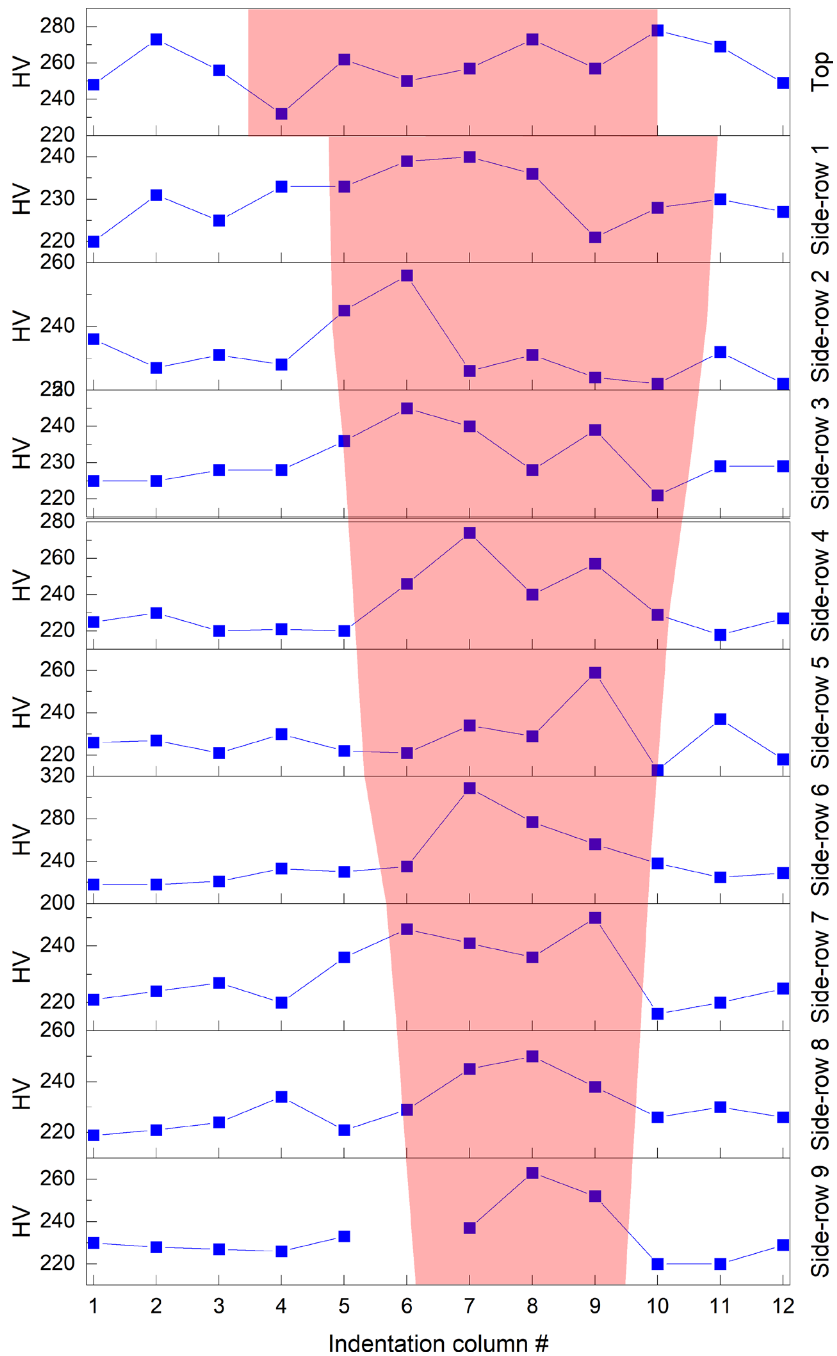

Figure 19. Hardness profiles on top and side surfaces of specimen 61-7143. The red highlighted region corresponds to the weld fusion zone.

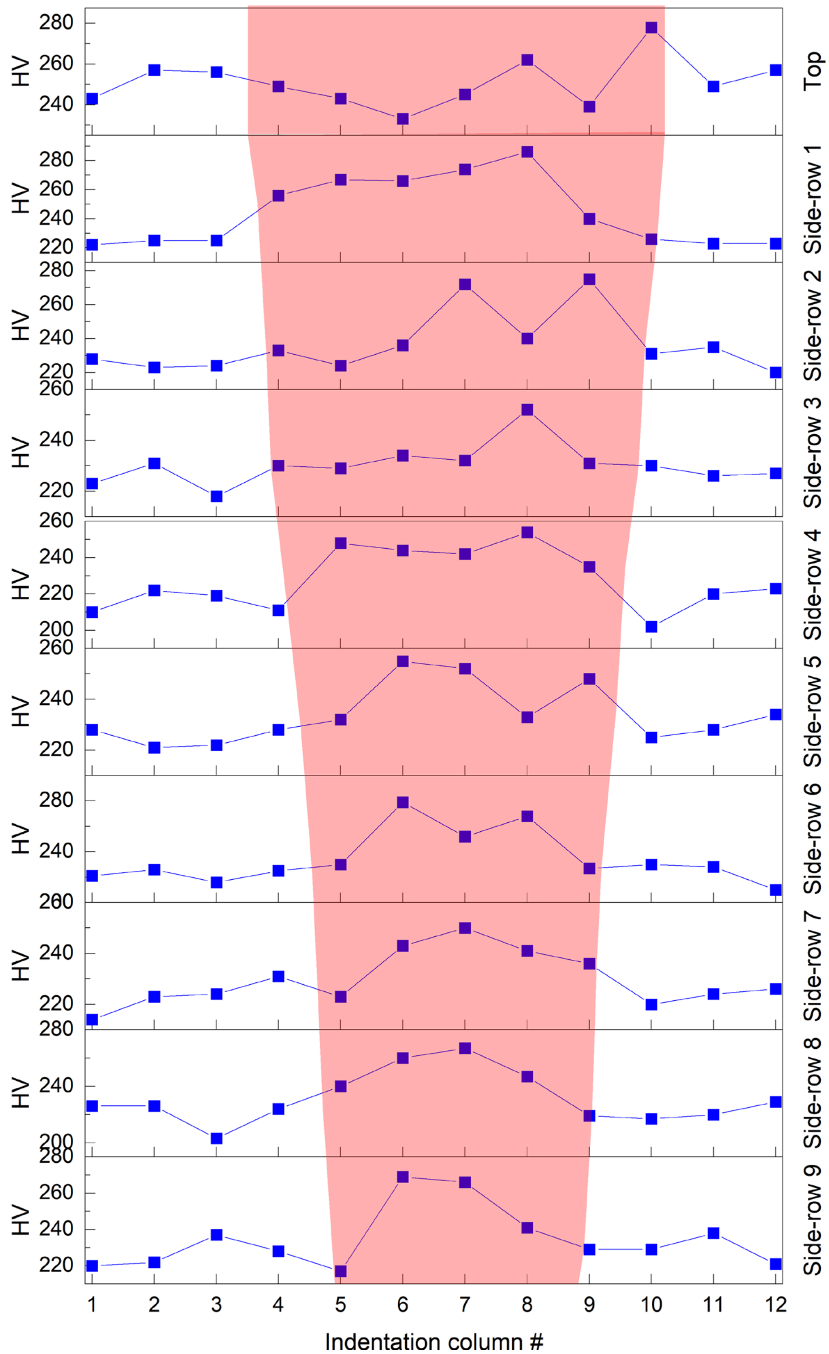

Figure 20. Hardness profiles on top and side surfaces of specimen 61-7180. The red highlighted region corresponds to the weld fusion zone.

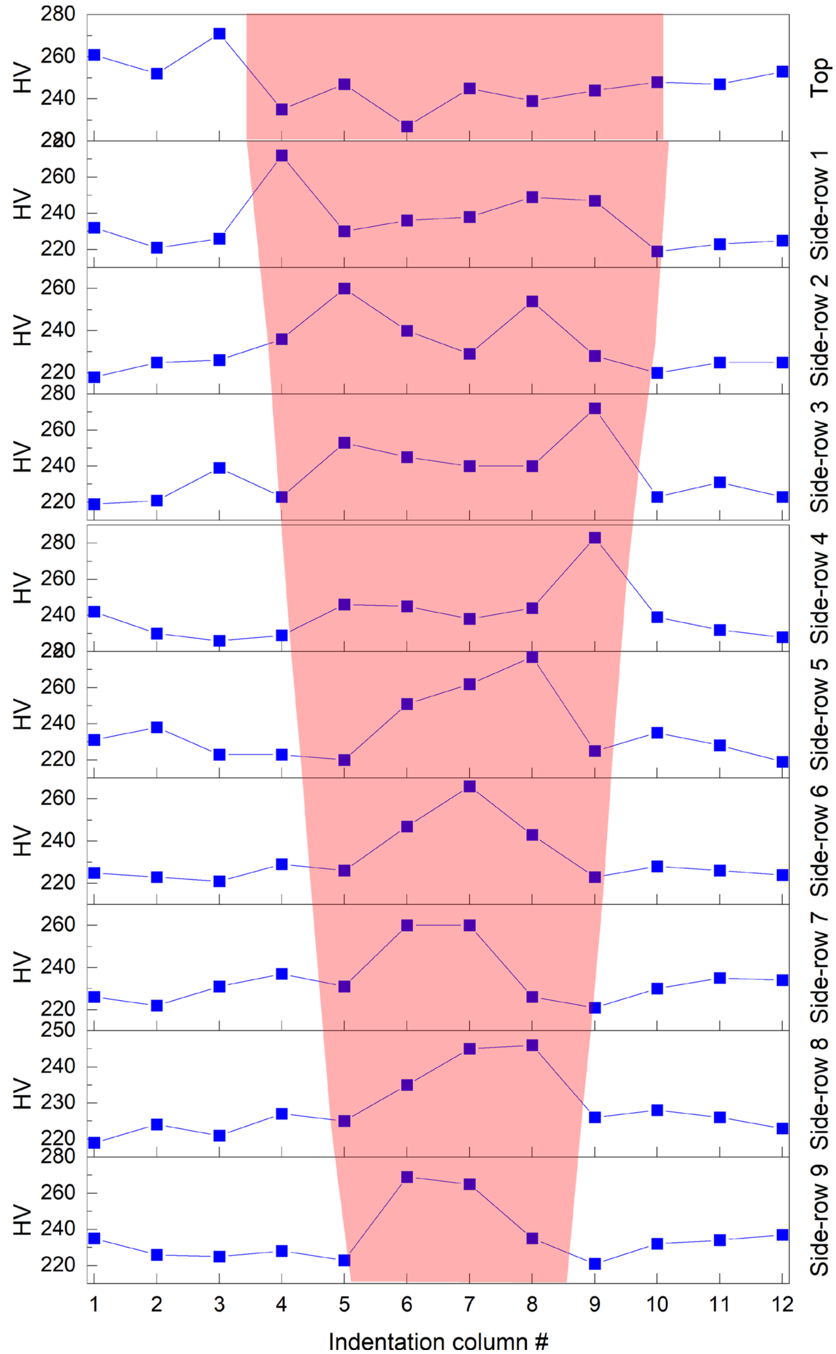

Figure 21. Hardness profiles on top and side surfaces of specimen 61-7181. The red highlighted region corresponds to the weld fusion zone.

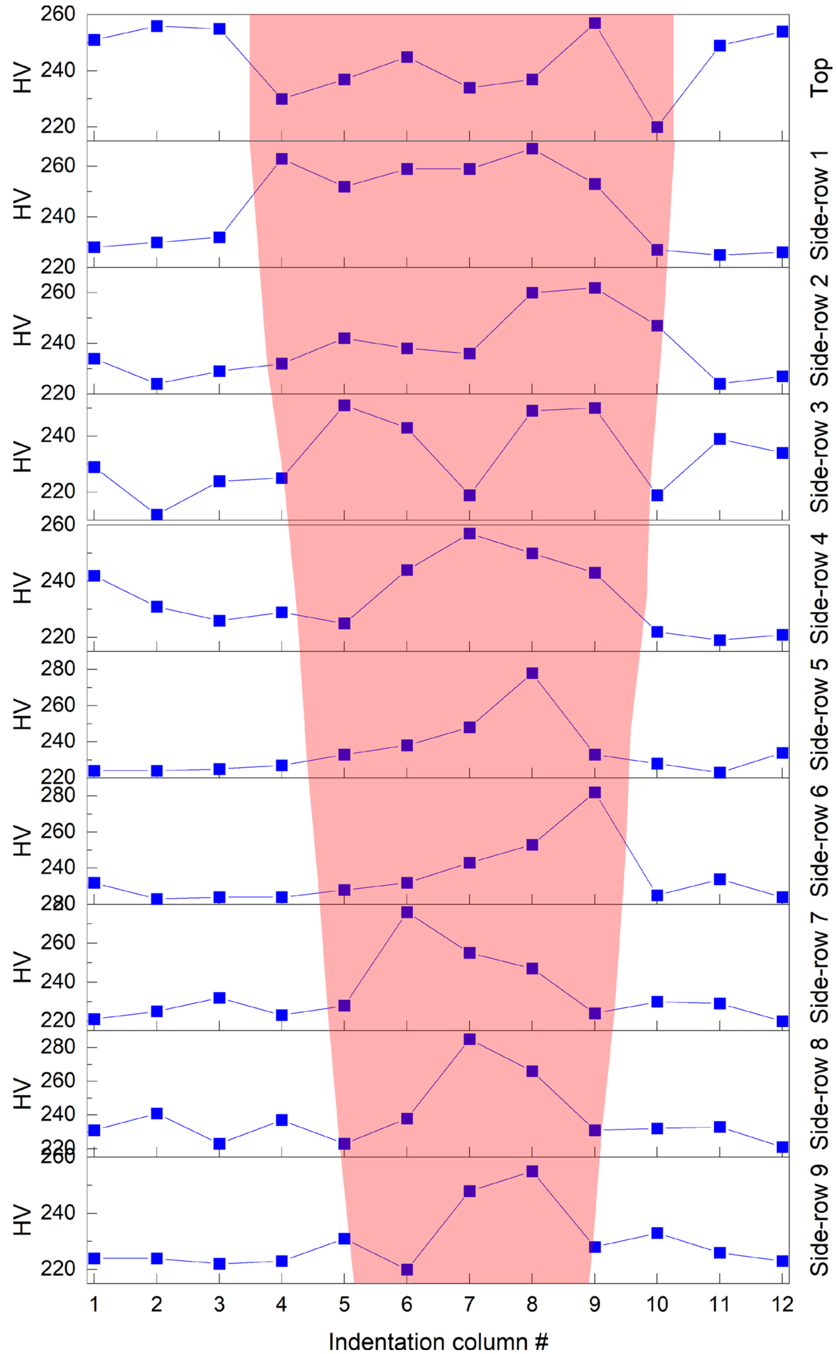

Figure 22. Hardness profiles on top and side surfaces of specimen 61-7194. The red highlighted region corresponds to the weld fusion zone.

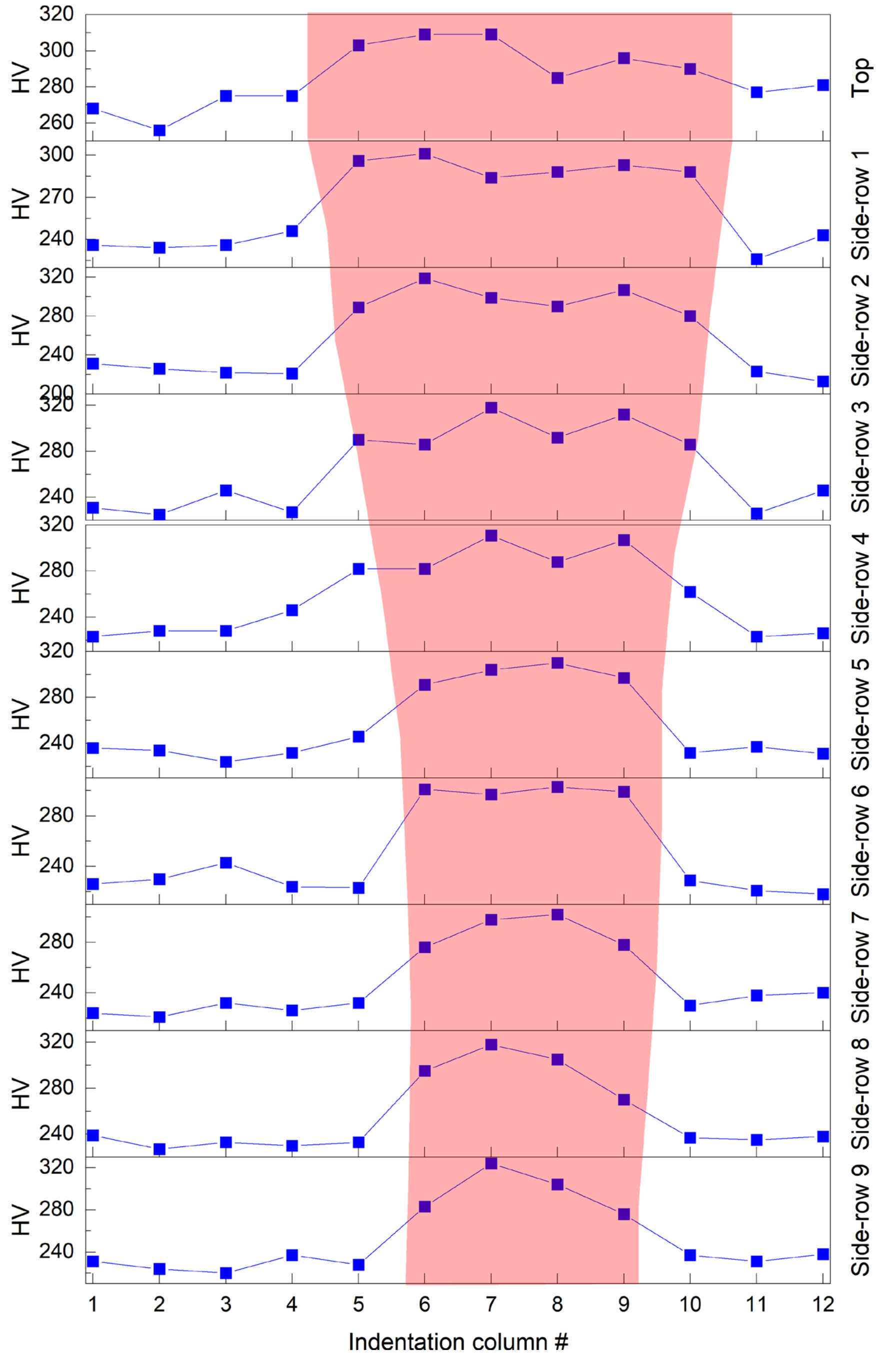

Figure 23. Hardness profiles on top and side surfaces of specimen 61-7270. The red highlighted region corresponds to the weld fusion zone.

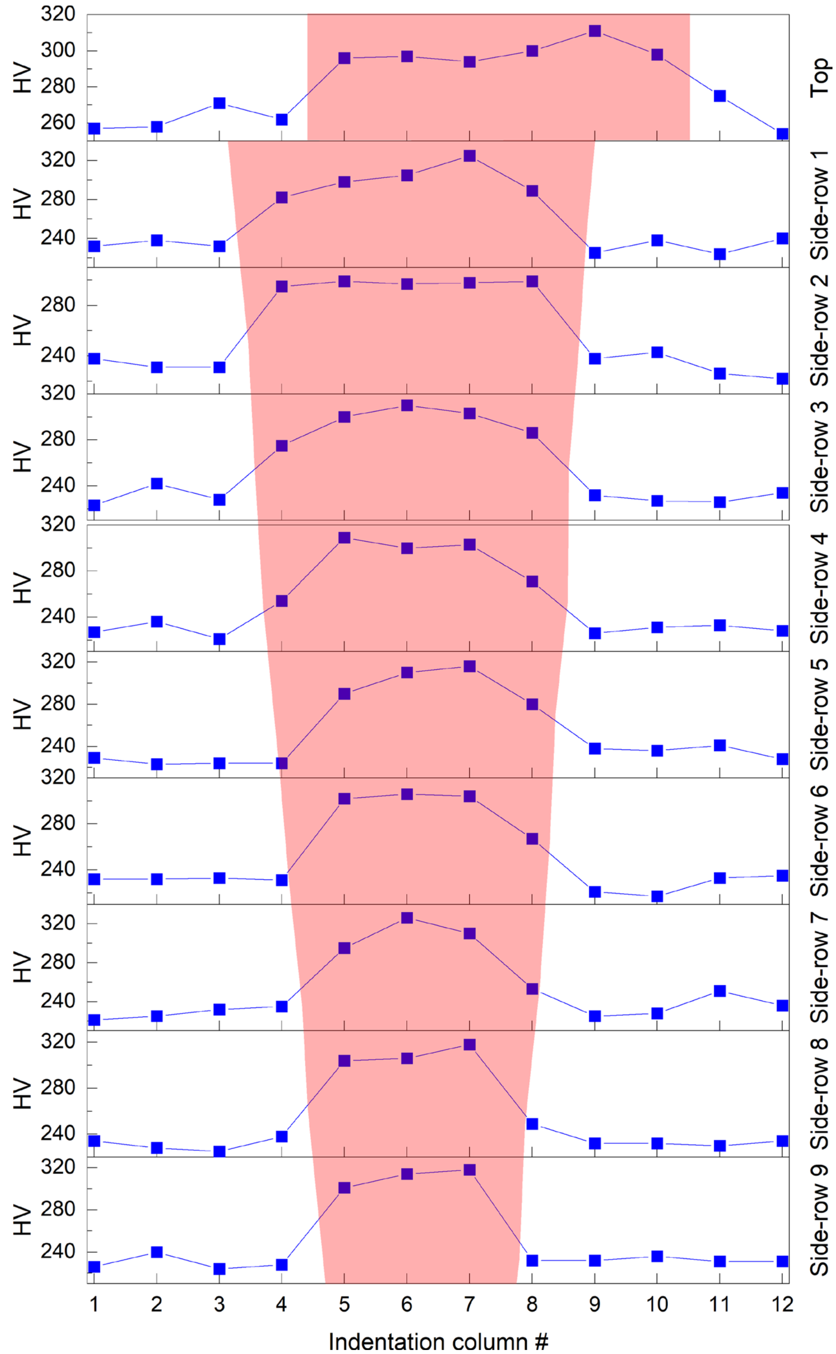

Figure 24. Hardness profiles on top and side surfaces of specimen 61-7279. The red highlighted region corresponds to the weld fusion zone.

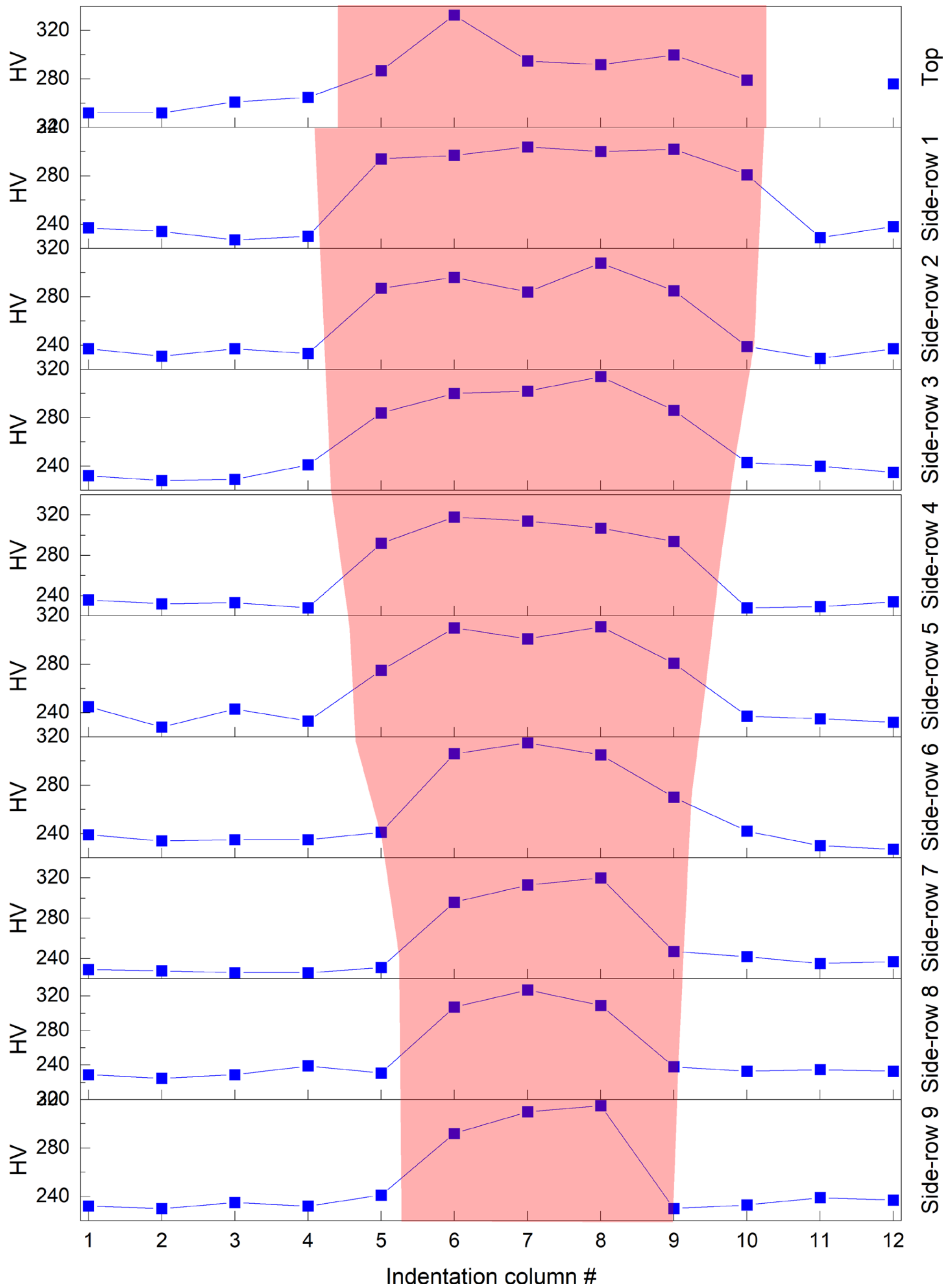

Figure 25. Hardness profiles on top and side surfaces of specimen 61-7284. The red highlighted region corresponds to the weld fusion zone.

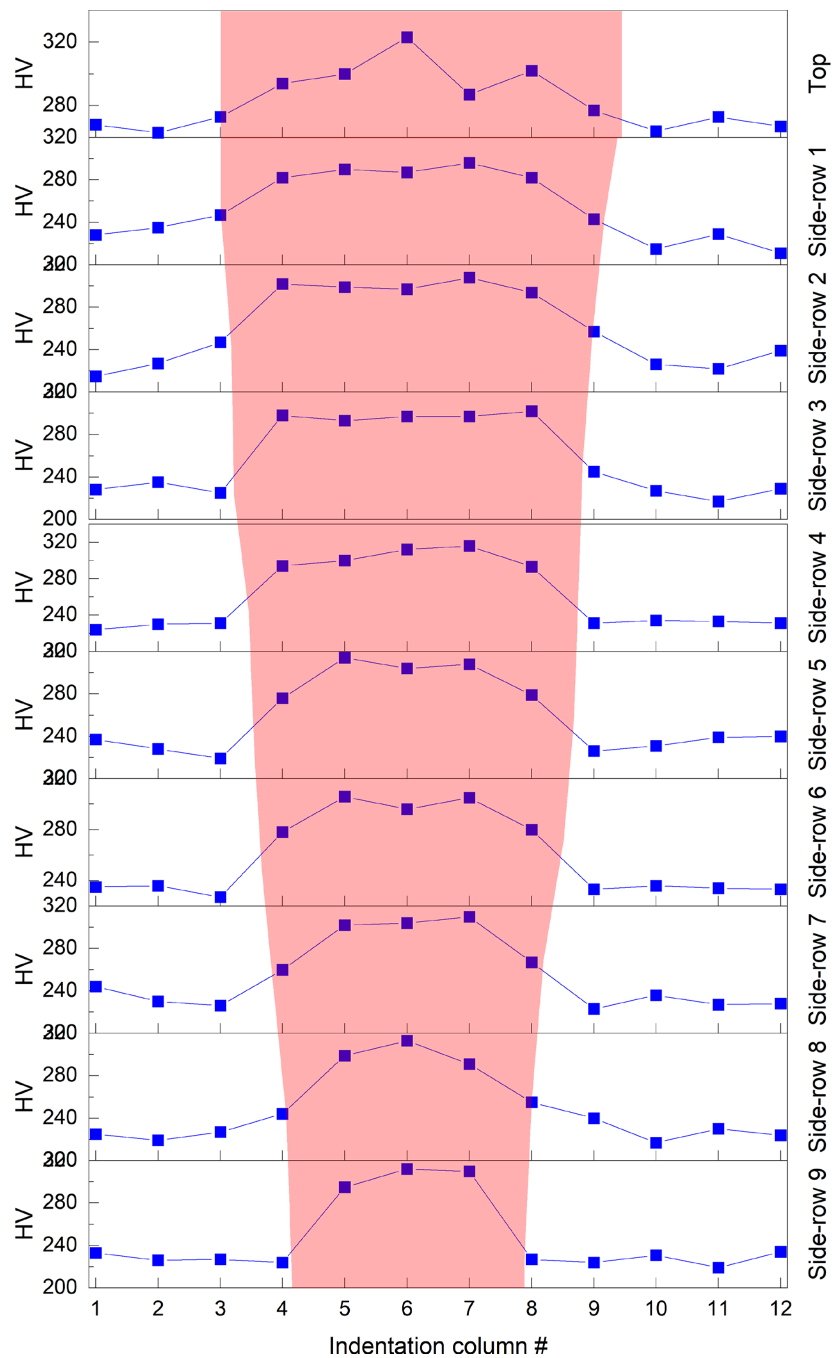

Figure 26. Hardness profiles on top and side surfaces of specimen 61-7304. The red highlighted region corresponds to the weld fusion zone.

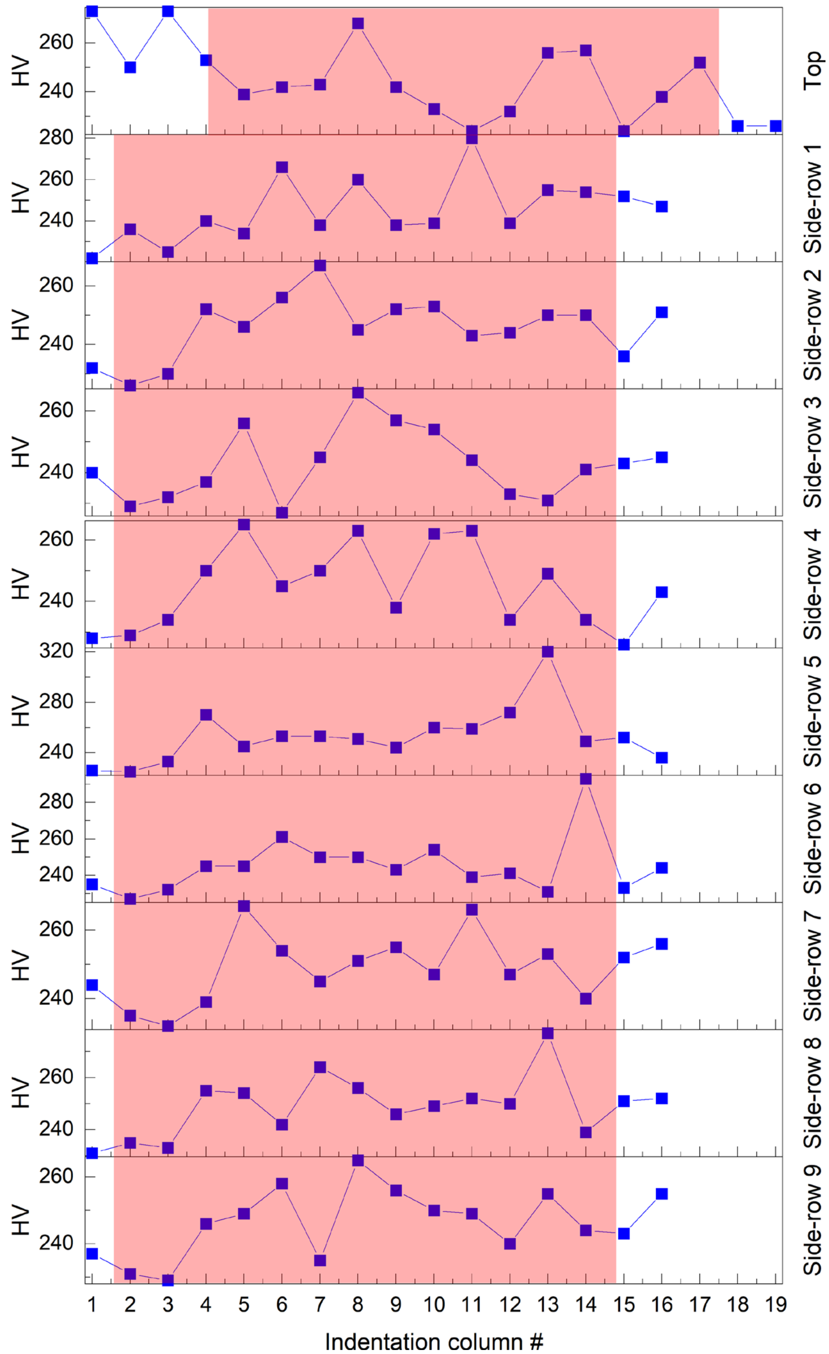

Figure 27. Hardness profiles on top and side surfaces of specimen 61-7357. The red highlighted region corresponds to the weld fusion zone.

2.2 MECHANICAL TEST RESULTS

2.2.1 Set #1: Specimens Tested at Elevated Strain Rate (0.01 s^{-1})

The initial set of experiments was performed at an elevated strain rate (0.01 s^{-1}) instead of a nominal desired value of 0.001 s^{-1}. The test conditions and mechanical properties of the tested specimens are summarized in Table 11. The strength level for specimens tested at room temperature was higher than those tested at elevated temperatures. Regardless of the initial weldment microstructure, all specimens have a small uniform elongation (UE) value below 1%–1.5%. The total elongation (TE) value was observed to depend strongly on the test temperature; room temperature tests showed smaller TE values than those of the elevated temperature tests.

Table 11. Testing conditions and mechanical properties for specimens tested at the strain rate of 0.01 s^{-1}

Specimen ID	Weldment structure	Test temperature (°C)	Strain rate (s^{-1})	YS (MPa)	UTS (MPa)	UE (%)	TE (%)
61-7143-2	Blocky Alpha	20	0.01	719.34	719.34	0.08	0.08
61-7143-3	Blocky Alpha	20	0.01	779.94	787.14	0.48	0.48
61-7180-3	Blocky Alpha	20	0.01	751.54	757.49	0.14	1.29
61-7180-4	Blocky Alpha	315	0.01	464.58	468.6	0.33	6.63
61-7181-3	Blocky Alpha	20	0.01	735.82	742.09	0.31	0.55
61-7181-4	Blocky Alpha	315	0.01	428.83	434.57	0.32	8.75
61-7194-2	Blocky Alpha	20	0.01	663.55	720.71	0.77	1.38
61-7194-3	Blocky Alpha	315	0.01	431.22	433.95	0.36	8.26
61-7270-3	Precursor	20	0.01	727.03	837.66	0.71	4.12
61-7270-4	Precursor	20	0.01	787.51	861.95	0.66	4.26
61-7279-2	Precursor	20	0.01	767.66	852.16	0.77	6.49
61-7279-4	Precursor	315	0.01	449.65	483.84	0.44	8.84
61-7284-2	Precursor	20	0.01	818.53	871.1	0.59	5.57
61-7284-3	Precursor	315	0.01	474.49	495.68	0.49	6.45
61-7304-2	Precursor	20	0.01	844.16	868.49	0.45	3.65
61-7304-3	Precursor	315	0.01	485.01	485.43	0.15	7.2
61-7357-1	Widmanstätten	20	0.01	744.57	846.97	0.89	5.39
61-7357-2	Widmanstätten	20	0.01	622.47	800.49	1.4	1.4

TE = total elongation, UE = uniform elongation, UTS = ultimate tensile stress, YS = yield stress

2.2.2 Set #2: Specimens Tested at a Strain Rate of 0.001 s^{-1}

The second set of specimens was tested using a nominal strain rate of $10^{-3} \cdot s^{-1}$. The results are summarized in Table 12. The results clearly show that all irradiated specimens showed UE <1% (neck developed almost immediately after yield stress [YS]). A well-developed neck was observed for all specimens, suggesting good, localized ductility. Note that the UE value is low for some specimens—that is, less than 0.5% (e.g., 61-7237-2, 61-7238-2, 61-7243-2). Thus, the YS and ultimate tensile stress (UTS) values obtained from the engineering curve are very close.

Table 12. Testing conditions and mechanical properties for specimens tested at the strain rate of 0.001 s^{-1}

Specimen ID	Weldment structure	Test temperature (°C)	Strain rate (s^{-1})	YS (MPa)	UTS (MPa)	UE (%)	TE (%)
61-7143-4	Blocky Alpha	20	0.001	718.04	755.4	0.85	1.37
61-7180-2	Blocky Alpha	20	0.001	713.72	766.58	0.94	1.59
61-7270-2	Precursor	20	0.001	809.44	849.64	0.5	4.59
61-7279-3	Precursor	20	0.001	725.31	773.17	0.55	6.05
61-7357-3	Widmanstätten	20	0.001	723.42	807.77	1.07	5.1
61-7284-4	Precursor	315	0.001	403.55	468.57	1.1	8.81
61-7304-4 [1]	Precursor	315	0.001	266.92	329.09	4.89	24.18
61-7194-4 [2]	Blocky Alpha	315	0.001	247.97	270.32	0.95	8.2
61-7181-5	Blocky Alpha	315	0.001	373.97	376.13	0.37	8.48

[1] Compromised test (specimen rotated in the grips)
[2] Deformation developed very close to the specimen head (likely, soft material from HAZ started to deform first)
TE = total elongation, UE = uniform elongation, UTS = ultimate tensile stress, YS = yield stress

2.2.3 Set #3: Specimens Cut from the Bottom Portion of the Weldments

To enhance the statistics, an additional set of specimens was produced from the weldment bottom portions (see Section 1.4). To underline the different origins and orientations of these specimens, "R"-char ("rotated") was added to the specimen IDs. Compared with Sets #1 and #2, specimens within Set #3 showed, in general, lower strength levels and higher elongation values. A survey of the deformed specimens showed that plastic deformation, necking, and fracturing developed close to the specimen heads in most cases, inside the HAZ (i.e., outside the weldment). The test results are summarized in Table 13.

Table 13. Testing conditions and mechanical test results for specimens cut from the weldment bottom portions

Specimen ID	Weldment structure	Test temperature (°C)	Strain rate (s^{-1})	YS (MPa)	UTS (MPa)	UE (%)	TE (%)
61-7180-R3	Blocky Alpha	315	0.001	385.84	449.11	2.92	23.86
61-7270-R3	Precursor	315	0.001	356.59	451.32	1.55	16.64
61-7270-R4	Precursor	315	0.001	416.38	480.03	3.24	17.68
61-7304-R3	Precursor	315	0.001	426.01	514.99	3.81	17.76
61-7181-R3	Blocky Alpha	20	0.001	688.56	798.91	2.98	7.75
61-7181-R4	Blocky Alpha	20	0.001	672.18	828.85	3.66	7.02
61-7194-R3	Blocky Alpha	20	0.001	677.9	838.18	4.21	7.37
61-7194-R4	Blocky Alpha	20	0.001	644.35	804.52	3.82	10.18
61-7279-R3	Precursor	20	0.001	710.44	814.12	2.76	6.65
61-7279-R4	Precursor	20	0.001	693.01	816.95	3.73	8.89
61-7284-R3	Precursor	20	0.001	676.29	804.84	2.63	5.62
61-7284-R4	Precursor	20	0.001	710.81	850.53	3.88	6.85

TE = total elongation, UE = uniform elongation, UTS = ultimate tensile stress, YS = yield stress

2.3 PRELIMINARY ANALYSIS OF DIGITAL IMAGE CORRELATION DATA

Irradiated materials are sensitive to localized deformation, and necking often develops upon reaching YS. Digital images were recorded during the mechanical test to investigate the strain-induced deformation processes in the irradiated weldments and to assess the localized deformation.

The images were recorded using a telecentric lens with an appropriate working distance. The lenses provided an optic resolution of ~3.5 μm per pixel. The images were recorded with 1 Hz frequency; this value compromises data amounts and the ability to resolve strain-induced processes. In most cases, the 1 Hz imaging frequency is sufficient for testing at the strain rate of 0.001 s^{-1} but does not provide enough data for specimens tested at 0.01 s^{-1}. For specimens tested at elevated strain rates, the results may give strain distribution for several strain levels but may not give detailed kinetics of the process. Table 14 lists all tested specimens, identifies whether digital image correlation (DIC) images were collected, and estimates DIC image quality.

Table 14. Assessment of DIC data and strain-induced phenomena (specimens are shown in approximately chronological order)

Specimen ID	DIC data	Notes
61-7101-3	NA	
61-7101-2	NA	
61-7143-2	Acceptable	
61-7143-3	Acceptable	
61-7180-3	NA	
61-7180-4	NA	
61-7181-3	NA	
61-7181-4	NA	
61-7194-2	Good	Band pattern may be visible in the last image prior to fracture
61-7194-3	NA	
61-7270-3	NA	
61-7270-4	NA	
61-7279-2	Good	Well-developed neck
61-7279-4	NA	
61-7284-2	Good	Well-developed neck
61-7284-3	NA	
61-7304-2	Good	
61-7304-3	NA	
61-7357-1	Good	Well-developed neck
61-7357-2	Good	Just a few images
61-7143-4	Good	
61-7180-2	Good	Interesting semitransparent last image (quick fracture)
61-7270-2	Acceptable	Well-developed neck in the HAZ
61-7279-3	Acceptable	Necking is visible
61-7357-3	Acceptable	Specimen rotated in the grips later in the test
61-7284-4	Poor	Paint layer cracking in the neck
61-7304-4	Failed test	Abnormal (specimen rotated in the grips)

Table 14. Assessment of DIC data and strain-induced phenomena (specimens are shown in approximately chronological order) (continued)

Specimen ID	DIC data	Notes
61-7194-4	Acceptable	Abnormal (gauge damage)
61-7181-5	Poor	Very long fracture (ductile tearing at almost zero loads)
61-7180-R3	Acceptable	Very interesting pattern of shear bands
61-7270-R3	Good	Strong neck, developing as an intersection of two deformation bands
61-7270-R4	Acceptable	The very strong shear band, followed by pronounced necking
61-7304-R3	Good	Well-developed neck in HAZ
61-7181-R3	Acceptable	
61-7181-R4	Acceptable	Well-pronounced shear bands
61-7194-R3	Good	Strong shear band after the ultimate stress point
61-7194-R4	Acceptable	Well-developed neck in the HAZ
61-7279-R3	Acceptable	Well-developed shear band
61-7279-R4	Acceptable	Deformation in soft heads and well-developed shear band
61-7284-R3	Good	Well-developed shear band
61-7284-R4	Acceptable	Shear bands in the HAZ

HAZ = heat-affected zone, NA = not applicable

2.3.1 61-7143-4 Specimen

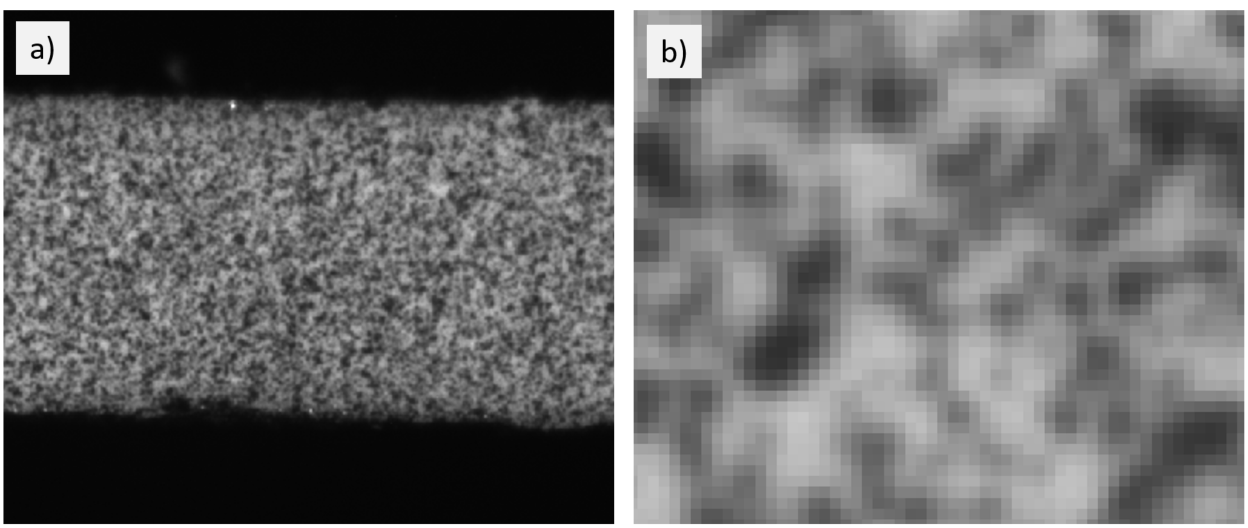

Figure 28. (a) General view of the painted specimen gauge (tensile direction is horizontal) and (b) magnified view of the pattern showing the speckle size and density.

A full-scale investigation or assessment of the strain-induced phenomena was out of this work's scope. Only a brief analysis was performed, and one typical specimen from the weldment's top will be discussed in what follows. Figure 28(a) shows a general view of the painted specimen gauge, and Figure 28(b) shows a magnified view of the DIC pattern. The pattern quality varied between different specimens, which is usually slightly lower for specimens tested at elevated temperatures because the multilayer glass window influences imaging conditions.

Figure 29(a) shows a strain distribution along the deformed specimen surface directly before fracture, and Figure 29(b) shows displacement and load for the analyzed image. The figure shows that most of the specimen gauge portion experienced very weak strains (mostly elastic). Deformation is localized in one small area (neck), and very limited, if any, plastic deformation occurs outside this area.

The neck has a complex structure and consists of a few intersecting deformation bands. The bands interact with each other and appear to be inclined at some angle, with respect to the tensile axis.

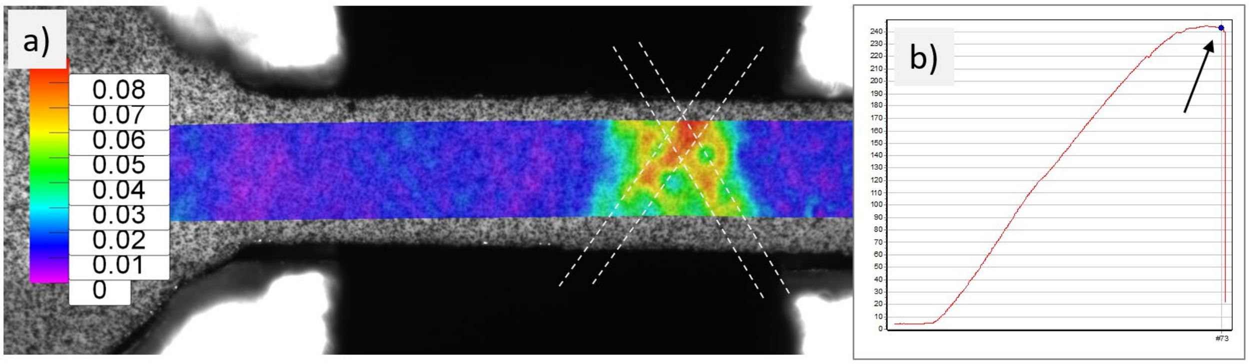

Figure 29. (a) Strain field (elastic + plastic) at the surface of 61-7143-4 specimen directly before fracture and (b) tensile diagram with an arrow showing the location of the last taken image (in load displacement coordinates). Most likely, the neck developed because of the evolution and interaction of several deformation bands (two of these are shown by dashed lines).

Figure 30 shows the microstructure of the 61-7143 weldment. The figure shows elongated columnar grains in the weldment middle, much smaller grains close to the weldment boundary, and fine grain structure in the parent material. Variations in grain size may influence active deformation mechanisms; thus, large, coarse grains in the weldment middle make twinning more favorable than in areas with fine grains. The exact microstructure of the tensile specimen is unknown. However, an overlap of the strain map (Figure 29) and grain structure suggests that the neck formed and deformation bands developed close to the weldment middle in the area with columnar grains.

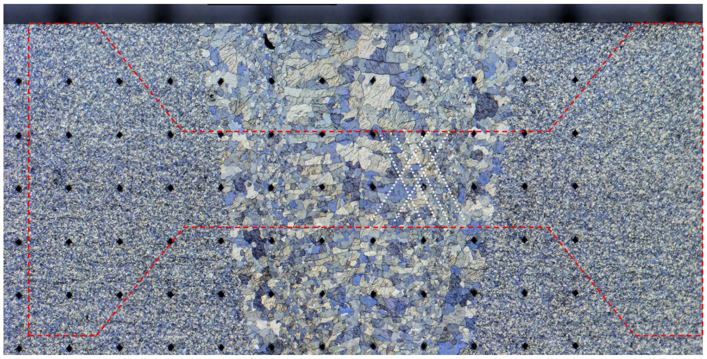

Figure 30. Microstructure of the 61-7143 weldment and an approximate location (red dashed contour) of the tensile specimen cut from this weldment. The dashed lines show the approximate locations of the observed deformation bands (also see Figure 29).

3. SUMMARY AND CONCLUSIONS

This report summarizes the experimental results on microstructure, microhardness, and mechanical properties of Zr alloy weldments irradiated by neutrons.

4. ACKNOWLEDGMENTS

The authors would like to thank ORNL LAMDA staff (P. Tedder, S. Curlin, A. Godfrey, and K. Everett) for help with specimen handling, preparation, and testing; Dr. T. S. Byun (ORNL) for reviewing the report; and J. Hingtgen (ORNL) for help with document preparation.

REFERENCES

1. Maxim N. Gussev, Richard H. Howard, Kurt A. Terrani, and Kevin G. Field. “Sub-size tensile specimen design for in-reactor irradiation and post-irradiation testing.” *Nuclear Engineering and Design* 320 (2017): 298–308.
2. Maxim N. Gussev, Jeremy Busby, Kevin Field, Mikhail Sokolov, and Sean Gray. “Role of scale factor during tensile testing of small specimens.” *Small Specimen Test Techniques: 6th Volume*. ASTM International (2015).
3. Maxim N. Gussev, Kevin G. Field, and Yukinori Yamamoto. “Design, properties, and weldability of advanced oxidation resistant FeCrAl alloys.” *Materials & Design* 129 (2017): 227–238.
4. Maxim N. Gussev, Ercan Cakmak, and Kevin G. Field. “Impact of neutron irradiation on mechanical performance of FeCrAl alloy laser-beam weldments.” *Journal of Nuclear Materials* 504 (2018): 221–233.